SCIENTIFIC COMMITTEE
TWENTY-SECOND REGULAR SESSION
11-19 August 2026
Apia, Samoa (Hybrid)

INVESTIGATION OF SINGLE-REGION FLEETS-AS-AREAS MODELS FOR BIGEYE AND YELLOWFIN TUNA IN THE WESTERN AND CENTRAL PACIFIC OCEAN

WCPFC-SC22-2026-SA-IP09
27 July 2026

Submitted by

John Hampton[1,2,3], Thom Teears[1], Khuyan Kim[1], and Paul Hamer[1]

[1] Oceanic Fisheries Programme of the Pacific Community (SPC)
[2] Thunnidae Consulting, Brisbane, Australia
[3] University of Wollongong, Wollongong, Australia

Investigation of single-region fleets-as-areas models for bigeye and yellowfin tuna in the western and central Pacific Ocean

John Hampton, Thomas Teears, Kyuhan Kim and Paul Hamer

Executive summary

Following requests from Scientific Committee delegates and the 2026 SPC Pre-Assessment Workshop to explore simpler alternatives to the multi-region spatial stock assessments, this paper investigates single-region ("fleets-as-areas") models for bigeye and yellowfin tuna in the western and central Pacific Ocean, run alongside the main 2026 assessments. Each model represents the WCPO as a single, well-mixed population disaggregated by 40 quarterly age classes over 1952–2024, using the same catch, length-frequency and conditional age-at-length (CAAL) data as the corresponding five-region 2026 assessments, but with a single WCPO-wide abundance index and more flexible, time-invariant selectivity curves in place of spatial movement and recruitment-distribution parameters.

Both models converged cleanly, with low maximum gradients, positive definite Hessians, no material parameter confounding, and robustness to jittered starting values, at least in terms of assessment-related estimates. Both models fitted the abundance indices and aggregate length-frequency data acceptably well, although neither could capture fine-scale temporal and modal structure in the length data. Conditional age-at-length residuals showed systematic patterns by region and fish size for both species. Age-structured production model (ASPM) and catch-curve diagnostics indicated that the bigeye tuna model's population scale and trends are reasonably well informed by, and consistent between, the abundance index and the size/age composition data. The yellowfin tuna model showed a less consistent picture, with the constant-recruitment ASPM under-estimating population scale and a clearer conflict between the length-frequency data and the CAAL/CPUE data in the likelihood profile. Both the bigeye and yellowfin models exhibited significant retrospective bias (Mohn's ρ exceeding 0.2 in absolute value for spawning biomass, depletion and fishing mortality), consistently in the direction of increasingly pessimistic stock status estimates with successive removal of terminal years.

Estimated growth, recruitment and biomass patterns from the single-region models are broadly consistent with the corresponding 2023 spatial assessments (noting that the 2026 assessment results were unavailable at the time of writing), although the estimated scaling of bigeye tuna biomass is around 25% lower and that of yellowfin tuna is higher, particularly before 1990. Estimated asymptotic length for both species is around 4 cm lower than in 2023, most likely related to the expanded CAAL data sets now available.

Overall, the single-region models are numerically robust and provide a useful, more readily diagnosed complement to the spatial assessments, particularly for bigeye tuna. However, the regional residual patterns in the CAAL data, data conflicts (especially for yellowfin tuna) and

significant retrospective bias identified here indicate that spatial aggregation introduces real misspecification, and the single-region models are not yet a viable substitute for the spatially-structured assessments used to provide management advice to WCPFC. In particular, it is possible that the single-region models estimate a more pessimistic picture of stock status than the spatial assessment models because they cannot recognise that large portions of the WCPO outside of the equatorial areas have much lower levels of exploitation despite there being substantial stocks in those lightly exploited areas. The single-region models, by their nature, are likely to be more indicative of exploitation conditions in the tropical areas, where the majority of the data originate.

A potential refinement identified for future work is to allow selectivity to vary through time. Also, the CAAL results in particular highlight the regional heterogeneity in growth, which should be a high priority for the development of future integrated spatial stock assessment models.

Introduction

Tuna stock assessments conducted by SPC have usually adopted a spatial approach, dividing the western and central Pacific Ocean (or the WCPFC Convention Area) into up to nine model regions. That approach has been taken so that heterogeneity in the spatial distribution of tuna populations and their exploitation characteristics can be better characterised. Such spatial models can also provide potentially more nuanced management advice to WCPFC, that reflects, for example, different levels of stock depletion in different regions. However, spatial models are inevitably more complex – they require parameters to describe movement of fish among regions and the distribution of recruitment among regions for each time step of the model. Such complexity creates greater demands on the available data and sometimes makes the models harder to fit. In recent years there has been increased attention given to evaluating the performance of stock assessment models through detailed examination of model diagnostics (Carvalho et al., 2021). As these techniques have been more routinely incorporated into SPC spatial stock assessments, issues such as data conflict, retrospective bias and sensitivity of models to parameter starting values have been regularly identified. This has led some Scientific Committee delegates to express the view that, at least in some cases, the spatial models are too complex and need to be simplified to improve the statistical properties of the models, including diagnostics such as those mentioned above. This view was reiterated at the 2026 SPC Pre-Assessment Workshop (Hamer, 2026), which requested that single-region fleets-as-areas models for bigeye and yellowfin tuna be explored, in conjunction with the 2026 assessments. This report documents those explorations for bigeye and yellowfin tuna in the western and central Pacific Ocean (WCPO) region. We also briefly explored single-region tropical models (where the majority of catches actually occur for both species), to compare certain aspects of the population dynamics.

Methods

Model configuration

The key features of the configuration of the WCPO single-region bigeye and yellowfin tuna models are:

1. The models comprise single WCPO-wide populations (Figure 1) that are disaggregated into 40 quarterly age classes. As noted, we also examine single-region models comprising only the tropical regions, denoted regions 2, 3 and 4 in Figure 1. The results of these models are provided in Appendix 1.
2. The model time window is 1952-2024, using quarterly time steps. 1952 is around the time that significant industrial exploitation of bigeye and yellowfin tuna began in the Pacific. Therefore, we have assumed unfished populations in 1952.
3. The fisheries defined for each model are specific to sub-regions (Figure 1), gear and in some cases nationality (Table 1, Table 2). The fisheries definitions and associated catch and length-frequency data are identical to those in the main 2026 assessments for these species (Kim et al., 2026; Magnussen et al., 2026), with the exception that single WCPO-wide abundance indices have been used. These were compiled from the global sdmTMB models for bigeye and yellowfin tuna as described by Teears et al. (2026).
4. The models are catch-conditioned, meaning that the observed catches are extracted from the population without observation error.
5. Tagging data were not included in the models, due to the WCPO-wide single area approach and the need to make unrealistic assumptions regarding tag mixing in this large area in order to include tagging data.
6. Fishery-specific selectivities were modelled as age-specific splines. More complexity in the shape of the selectivity curves was allowed compared to the respective spatially-structured stock assessment models. This is because selectivity in "fleets-as-areas" models represents both the intrinsic probability of a gear catching fish of a certain age if it is present (so-called "contact selectivity") and the availability of fish of that age in the spatial region in which the fishery operates. A full description of selectivity assumptions is provided in *Table 3*.
7. Growth was estimated internally in the model using the standard MFCL von Bertalanffy growth parameterisation – *L1* (mean length of the first age class), *L40* (mean length of the oldest age class) and the growth coefficient *k*. The distribution of length-at-age was modelled according to an age-class-specific mean and standard deviation of length-at-age, the latter dependent on two estimated parameters, *V1* and *V2*, providing a log-linear relationship between age-class and standard deviation. Parameters of recently updated weight-length relationships (Macdonald et al., 2023) have been specified in the models.
8. As in recent stock assessments of WCPO bigeye and yellowfin tuna, the proportion of the population considered to be reproductively mature was specified by length class based on available data on the reproductive biology of both species.
9. Natural mortality-at-age (M_a) was assumed to follow a Lorenzen shape whereby M_a is inversely proportional to the mean length-at-age. The scaling of M_a was fixed at the level estimated in the 2023 assessments (Day et al., 2023; Magnussen et al., 2023).
10. Recruitment was modelled using the orthogonal polynomial recruitment (OPR) approach, comprising a fully saturated year effect (but with a common year effect for the two terminal years) and a year-invariant seasonal effect. This approach allowed a substantial conservation of recruitment parameters to be estimated – 75 for the OPR structure compared to 292 using the standard "mean + deviates" approach. A comparison of the "mean+deviates" and OPR approaches for bigeye tuna is provided in Appendix 2.
11. The models were fitted using MFCL version 2.2.7.9 with a maximum gradient for convergence set at 1e-04.

Data inputs

Catch

The catches used in these models are identical to those used in the main assessments (Kim et al., 2026; Magnussen et al., 2026). Longline catches are specified in number of fish and the catches of other fisheries are given in weight (t). All catches are broken down by year and quarter. Catches by year (for convenience) and fishery (with catch number converted to catch weight where needed) are shown in Figure 2.

Abundance indices

Single WCPO-wide abundance indices derived from the global sdmTMB models for bigeye and yellowfin tuna (Teears et al. 2026) were used in the single-region models. As agreed at the 2026 Pre-Assessment Workshop (Hamer, 2026), a minimum effort-creep hypothesis was incorporated into the indices – effective effort was inflated by 1% per year from 1952 to 1976 (prior to the availability of vessel identity in the catch/effort data), and by 0.5% per year from 1977 to 2024 (during which time vessel identity was available and used in the global CPUE model). The abundance indices (including model fits) are shown in Figure 3.

Length-frequency data

The length-frequency (LF) data used for the extraction fisheries were identical to those used in the main assessments, consisting of spatial catch re-weighted aggregated samples of measured individual lengths and measured individual weights converted to lengths (see Peatman et al., 2026 for full details of data treatment). Standardised length frequencies were compiled into quarterly samples of 95 2-cm length bins ranging from 10-12 cm to 198-200 cm. For the bigeye and yellowfin tuna relative abundance indices, the same length-frequency source data were used but re-weighted using spatial standardised CPUE (Peatman et al., 2026; Teears et al., 2026) across the full WCPO model region. The time-aggregated standardised length-frequency data for all extraction fisheries and relative abundance indices are shown in Figure 4 and Figure 5 for bigeye and yellowfin tuna, respectively.

Conditional age-at-length data

The conditional age-at-length (CAAL) data sets used in the main assessments (Kim et al., 2026; Magnussen et al., 2026) were also used in the single-region WCPO models described in this paper. The data consisted of 2005 bigeye tuna and 1868 yellowfin tuna length-at-age observations from otolith readings, compiled into 181 and 182 fishery-specific quarterly age-frequencies within the 95 2-cm length bins for bigeye and yellowfin tuna, respectively.

Observation models

The observation models used for each of the data sources can be summarised as follows:

Catch data

As noted, catches are modelled without error and thus there is no log-likelihood component for the catch.

Abundance indices

A lognormal likelihood with an average coefficient of variation (CV) of 0.25 was used to fit the abundance indices.

Length-frequency data

A robust lognormal likelihood, with effective sample sizes at 0.05 x observed sample sizes and capped at 1000, was used to fit the LF data.

Conditional age-at-length data

A multinomial log-likelihood of age frequencies within length bins was used to fit the CAAL data.

Diagnostic methods

Model convergence

The models were considered to be converged if 1) a maximum parameter gradient of 1e-04 was achieved; 2) the Hessian matrix was positive definite; 3) the model fit could not be significantly improved by jittering the estimated parameters (Carvalho et al., 2021); (4) estimated parameters should not be on their bounds; or (5) be highly correlated with each other ($-0.9 > r > 0.9$).

Model fits

Plots of observed and predicted abundance index, length-frequency and conditional age-at-length data were examined, including residuals plots.

Age-Structured Production Model

ASPM diagnostics (Carvalho et al., 2021; Maunder and Piner, 2015; Minte-Vera et al., 2017) for the both models were estimated by 1) fixing growth and selectivity parameters at their estimated values; 2) removing the LF and CAAL data from the model, leaving only the abundance indices as data to be fitted; 3) setting all log recruitment deviations to a fixed value of 0; and 4) re-fitting the model estimating only the population scaling parameters. A comparison of biomass and depletion scaling and trends estimated by the ASPM and the full model gives an indication of the extent to which these estimates are informed by the abundance indices only. A second version of the ASPM, in which recruitment deviations were estimated, was also run.

Catch Curve Analysis (CCA)

A CCA is essentially the reverse of the ASPM, whereby the abundance index data are removed from the model and all parameter estimation retained. The CCA indicates the information on population trends and scaling provided by the LF and CAAL data.

Likelihood profiles

A likelihood profile over a metric related to population scale is frequently used to evaluate conflict among data types. In this assessment, we profiled on the estimated population biomass averaged over the full model period (1952-2024) and examined the response of the likelihood of each data type (and their components). Ideally, we would like to see the negative log likelihood of each data component used in the model reaching a minimum at similar levels of average biomass.

Retrospective analysis

Retrospective analyses were undertaken as a general test of the stability of the models. A robust model, when rerun with data for the terminal year/s sequentially excluded (Cadigan and Farrell, 2005), should produce outputs that are variable across runs, and without a systematic pattern in either the scaling or time-series trends. The Mohn's ρ statistic (Mohn, 1999), a measure of the average relative bias of retrospective estimates, was computed from six successive data peels for recruitment, spawning biomass, spawning biomass depletion and annual fishing mortality to indicate whether significant retrospective bias was present in the models.

Jitter analysis

In a jitter analysis, the model is re-run from initial conditions a number of times with randomly selected starting values. We jittered the initial values of active parameters (bound-aware perturbations with a CV of 0.1) as they were activated in the phased estimation. Fixed parameters were not jittered. Due to time limitations, only 30 jitters were able to be undertaken for each of the models.

Results

Model diagnostics

Model convergence

The convergence properties of the models can be summarised as follows:

1. Both models converged with a maximum parameter gradient of < 1e04.
2. Both models produced a positive definite Hessian.
3. The jitter analyses indicated that both models were robust to the jittered starting values of estimated parameters.
4. For bigeye tuna, 10 of 232 estimated parameters were close to their lower bound. For yellowfin tuna, 12 of 243 parameters were estimated at a lower bound. In all cases, this involved selectivity spline coefficients, indicating some degree of parameter redundancy in both models.
5. Parameter correlation in the bigeye tuna model was minor, with only 3 of a possible 53592 correlations being >0.9 or <-0.9. For the yellowfin tuna model, only 2 of a possible 58806 correlations were >0.9 or <-0.9. Higher correlations tended to involve the selectivity spline coefficients within individual fisheries. Nevertheless, the correlations indicated that there is no serious confounding in either model.

Notwithstanding a small number of selectivity parameters being estimated close to their lower bound, we were satisfied overall with the convergence properties of the models.

Model fits

Both models were able to fit the abundance indices (CPUE data) acceptably well (Figure 3). Similarly, the LF data were well fitted in aggregate (Figure 4, Figure 5). However, the model fits to the LF data at the level of the quarterly observations, and given the single-region model structure, is unable to use locally variable recruitment, movement and other age-related processes to fit the fine structure of much of the data. An example is shown in Figure 6, for bigeye and yellowfin tuna LF in fishery 1. LL.WEST.1. There is considerable modal structure apparent in the data that is likely related to seasonal recruitment in the region of the fishery and limited mixing with the areas to the south. The model is not able to capture this sort of complexity because of the spatial simplicity of the single-region model. Also, since selectivity is assumed to be constant over time, there is considerable lack of fit to the temporal variability of the LF data (Figure 7, Figure 8).

Fits and residuals plots for the CAAL data are shown in Figure 9 and Figure 10, respectively, for bigeye tuna and in Figure 11 and Figure 12, respectively, for yellowfin tuna. For bigeye tuna, the fits and residuals look reasonable overall, but there are some noticeable residual patterns for the bigeye 120-150 cm, including:

- A surplus of negative residuals for bigeye >120 cm (observed ages at a given length less than predicted by the model) for data sampled from fisheries in region 1;
- Surpluses of positive residuals for larger bigeye for data sampled from fisheries in regions 2, 3 and to some extent 5.

For yellowfin tuna, the aggregate fit and residuals are reasonable for fish <130 cm, but as for bigeye tuna there are noticeable patterns by region and by size, including:

- A surplus of negative residuals for yellowfin >100 cm for data sampled from the fisheries in region 1;
- A surplus of positive residuals for yellowfin >130 cm for data sampled from the fisheries in region 2;
- A surplus of positive residuals over most of the size range for yellowfin sampled from the fisheries in region 3;
- A surplus of positive residuals for yellowfin >130 cm sampled from the fisheries in regions 4 and 5.

Age-structured production models

Two versions of the ASPM were fitted, one without and one with estimated recruitment variability. In the first, only population scale is being estimated, informed only by the CPUE data. For bigeye tuna, the mean recruitment, SB and SB depletion are scaled reasonably well compared to the diagnostic case model, indicating that the CPUE index is informing population scale (Figure 13). Some of the time series changes in SB and SB depletion are also captured, although SB is over-estimated through the middle part of the time series and under-estimated in the last 10 years compared to the diagnostic case. When the estimation of recruitment variability is included, the estimates of recruitment, SB and SB depletion track the diagnostic case model estimates more closely. This indicates the desirable property that population scaling is informed by the CPUE indices.

For yellowfin tuna (Figure 14), the constant recruitment ASPM under-estimates recruitment and SB scale to a greater extent, and this under-estimation is not ameliorated by including recruitment variability in the estimation.

Catch-curve analysis

The catch curve analysis for bigeye tuna, in which the model is fitted to the size composition and CAAL data only, shows very similar recruitment variability and trends compared to the diagnostic case model, albeit with slightly lower recruitment in the first 20 years and slightly higher in the final 20 years of the model period (Figure 15). These differences are magnified in the SB and SB depletion trends. For yellowfin tuna (Figure 16), the initial declines in recruitment, SB and SB depletion are greatly exaggerated in the CCA, but the estimates converge with those of the diagnostic case model in the second half of the time series.

Likelihood profiles

The likelihood profile for bigeye tuna (Figure 17) indicates that the three key data types (LF, CAAL and CPUE data) are providing, in aggregate, a consistent signal for population scale without any serious data conflict. When the LF and CAAL data are broken down by fishery type and by region, we do observe some discrepancies:

- The Indonesian + Philippines LF data prefer a higher population scale than the main longline and purse seine LF data;
- LF data from the fisheries in regions 3 and 5 prefer a lower population scale, whereas the fisheries in region 4 prefer a higher scale;
- The CAAL data sampled from fisheries in region 3 tend to prefer a higher population scale than the data originating from other regions.

For yellowfin tuna, the aggregate likelihood profile (Figure 18) shows noticeable data conflict, with the LF data preferring lower population scaling compared to the CAAL and CPUE data. The LF data broken down by fishery type exhibits reasonable consistency in terms of population scaling. For the LF data broken down by fishery region, the data from regions 1 and 5 prefer low population scale and the data from region 3 prefer high population scale. For the CAAL data, samples originating from longline catches are the most influential and provide strong evidence against lower levels of population. The CAAL data appear consistent when broken down by fisheries region, with the exception of samples originating from region 3 fisheries.

Retrospective analysis

The six-peel retrospective analyses for both bigeye and yellowfin tuna single-region models reveal significant retrospective bias for SB, SB depletion and fishing mortality (F), with the absolute values of Mohn's ρ statistic exceeding 0.2 in all cases (Figure 19, Table 4, Table 5). Recruitment, with Mohn's ρ statistics of -0.175 (bigeye) and -0.037 (yellowfin), is less affected. The direction of the bias is negative for SB and SB depletion and positive for F, indicating that successive peels produce more pessimistic outcomes in terms of stock status. This suggests that caution is warranted in interpreting particularly the most recent estimates, which risk being overly pessimistic.

Jitter analysis

For bigeye tuna 28 of the 30 jitter runs converged with a maximum gradient of <1E-3. The lowest objective function value among converged runs was -295,043.1, 5.9 units higher than the bigeye tuna reference model; no converged run improved on the reference model (Figure 20). This indicates the numerical stability of the model over the tested starting-value perturbations but does not demonstrate that the global minimum was found. The results of important derived quantities (SB depletion, SB, recruitment and fishing mortality) were closely matched to the reference model for all converged jitter runs.

For yellowfin tuna, all 30 jitter runs converged with a maximum gradient of <1E-3. The lowest objective function value among 30 runs was -374,146.9, 11.3 units lower than the reference model; 12 converged runs improved on the reference model (Figure 21). Multiple starting values diagnose sensitivity to local minima, but do not by themselves identify the global minimum. Despite some variability in the converged objective function values, estimates of important derived quantities were closely matched to the reference model for all jitter runs.

Parameter estimates

Growth, maturity and natural mortality

Estimates of the biological parameters of growth, maturity-at-age and natural mortality (M)-at-age are shown in Figure 22 for both species. Estimates of growth are similar to previous assessments, although there has been a reduction of approximately 4 cm in the estimates of asymptotic length of both species compared to the 2023 assessment estimates. This is likely a result of the expanded CAAL data sets that are now available. Maturity-at-length (panels D of

Figure 22) are fixed inputs and are identical to those from the 2023 assessments. The scaling of M was also fixed at the values estimated in the 2023 assessments, and therefore the M-at-age and maturity-at-age differ marginally from the 2023 assessments only through their relationships to the estimated growth.

Recruitment, spawning biomass and depletion

Estimates, and their 95% confidence intervals, of recruitment, SB and SB depletion are shown in Figure 23 for bigeye tuna and Figure 24 for yellowfin tuna. The pattern of bigeye tuna estimated recruitment (early decline, an increase and absence of strong trends post-1985) is similar to that estimated in the 2023 assessment (Day et al., 2023). However, the scaling is around 25% lower, which flows through to down-scaled estimates of SB and SB depletion. SB depletion of bigeye is estimated in this model to have reached around 0.2 by the late 2010s, and, like SB, is estimated to have dipped sharply in the last three years.

The pattern of yellowfin tuna recruitment (Figure 24) is also similar to that estimated in the 2023 assessment (Magnussen et al., 2023), with substantially higher initial estimates declining until about 1990, and a slightly increasing trend thereafter. The scaling of recruitment is somewhat higher in the current model, particularly pre-1990. As a result, the scale of SB is considerably higher in the current model compared to the 2023 assessment, although the estimates post-2000 are more similar. The recent levels of SB depletion estimated in the current model are in the range 0.5-0.55, compared to 0.4-0.45 in the 2023 assessment.

Fishing mortality

Fishing mortality by annual age groups are plotted by year and by decade in Figure 25 for bigeye tuna and Figure 26 for yellowfin tuna. Both figures indicate that the highest F's occur on one-year-olds, particularly since 1970 when the domestic fisheries of Philippines and Indonesia begin. F's for the older age groups have been reasonably constant since about 2000, but there are noticeable increases in the F of five-year-old yellowfin tuna and to some extent bigeye tuna in the most recent year. This is related to the higher catches of both species reported in the Indonesian and Philippines domestic handline fisheries (fisheries 14 and 15, respectively) in 2024.

Discussion

Viability of single-region models for bigeye and yellowfin tuna

Overall, the single-region fleets-as-areas models for both bigeye and yellowfin tuna are numerically well-behaved: both converged to a low maximum gradient with a positive definite Hessian and showed no material parameter confounding. While jittering produced a range of objective function values (a range of about 60 likelihood units in each case) and for yellowfin tuna 12 of the jitter runs improved on the objective function value of the reference model, the key model results were nonetheless robust to the perturbed starting values.

However, viability also needs to consider the validity of the population dynamics being represented, and the wider diagnostic suite gives a more mixed picture of viability. For bigeye tuna, the ASPM and CCA results track the diagnostic case reasonably closely, and the likelihood profile shows a broadly consistent signal for population scale across data types, suggesting that the single-region structure is capturing the major features of the population dynamics acceptably well. For yellowfin tuna, however, the ASPMs substantially under-estimate population scale even when recruitment variability is allowed, and the aggregate likelihood profile shows clear conflict between the LF data and the CAAL/CPUE data. This suggests that, at least for yellowfin tuna, the single WCPO population is being asked to reconcile signals that likely originate from spatially distinct sub-populations and fisheries, and that the single-region structure is less able to do this than it is for bigeye tuna.

Both species also show significant retrospective bias, with $|\rho| > 0.2$ for SB, SB depletion and F. Because this bias is consistently negative for biomass/depletion and positive for F, terminal-year estimates run some risk of appearing overly pessimistic, and any use of these models for management advice would need to explicitly account for this. On balance, the single-region models appear viable as a simplified diagnostic and exploratory tool that can usefully complement the spatial assessments, particularly for bigeye tuna, but the results do not yet support their use as a direct substitute for the spatially-structured assessments.

Impact of spatial aggregation on model misspecification and bias in assessment results

Several results point to spatial aggregation as a source of model misspecification in the single-region structure. The CAAL residuals for both species show clear regional patterns rather than being randomly distributed with respect to region: for bigeye tuna, fisheries in region 1 show a surplus of negative residuals for larger fish while fisheries in regions 2 and 3 show a surplus of positive residuals, and yellowfin tuna shows an even more pronounced set of region-specific patterns. Because the single-region model (in common with the current generation of spatially-structured integrated assessment models) must estimate one overall age/length relationship, it cannot accommodate genuine differences in the growth, or in the resulting age composition of catch at length, that exist among regions, and the CAAL residuals are essentially recording that unmodelled regional heterogeneity. There is also the possibility of some degree of conflict between the LF and CAAL data with respect to growth, particularly at the larger/older end of the size/age range. The residuals patterns overall show some evidence of non-von Bertalanffy growth, which requires further investigation.

The likelihood profiles provide further evidence of spatial misspecification. For bigeye tuna, the Indonesian and Philippines domestic fisheries LF and CAAL data prefer a distinctly higher population scale than the main longline and purse seine fisheries, and LF data from different regions prefer different scales entirely (regions 3 and 5 lower, region 4 higher). For yellowfin tuna, the pattern is stronger still, with LF data overall preferring a lower population scale than the CAAL and CPUE data and marked regional splits within the LF data (regions 1 and 5 low, region 3 high). These are likely the signatures of spatially heterogeneous population dynamics and exploitation being forced into a single, spatially-averaged population trajectory. Unfortunately, the five-region models utilising the same data were not available for comparison at the time of writing this paper. Direct comparison of results and diagnostics described above may reveal whether any of the issues described here, particularly for yellowfin tuna, are resolved by the spatial models.

Recall that tagging data were not included in the current models due to the need to make unrealistic assumptions regarding the mixing of tagged fish across the entire model domain. In the previous spatially-structured assessments, the tagging data for bigeye tuna in particular were influential in population scaling, with the likelihood profile indicating that the tagging data were constraining the population to lower levels than indicated by some other data components

(Day et al., 2023). In omitting the tagging data from the single-region model, we had anticipated that population scaling might increase; however this did not occur. This suggests that the down-scaling of the bigeye tuna population in the single-region model relative to the 2023 assessment may be more to do with the shift to a spatially homogeneous model than to the changed weighting of different data components, including removal of tagging data. In this respect, it is noteworthy that the results for bigeye tuna in terms of population scale and levels of SB depletion obtained here are largely consistent with previous “fleets-as-areas” models for WCPO bigeye tuna, e.g. Ducharme-Barth et al. (2020, 2026).

The inability of the single-region model to represent local recruitment seasonality and limited mixing is also evident in the length-frequency fits: the modal structure apparent in, for example, fishery 1 (LL.WEST.1) is likely to reflect seasonal recruitment and restricted mixing with fisheries further south, which a single well-mixed population cannot reproduce. It is possible that the significant retrospective bias identified in both models is connected to this same source of misspecification. The relative contribution of different regions and fisheries to total catch has shifted substantially over the assessment period – most obviously through the development of the Indonesian and Philippines domestic fisheries from the 1970s onward, and their further expansion in the most recent years – and a single-region model has no mechanism to track a shifting spatial footprint of exploitation over time. As the mix of fisheries contributing data changes through time, so too does the compromise population trajectory that best fits the aggregated data, which is a plausible driver of the systematic retrospective patterns observed.

Potential improvements to the current models

Several relatively modest changes to the current model configuration could plausibly improve the diagnostic performance of the single-region models without reintroducing full spatial complexity. Given the regional conflicts identified in the likelihood profiles, down-weighting the fisheries data sets most strongly implicated in conflicting scale signals – particularly the yellowfin LF data and the region 3 CAAL data for both species – may help reconcile the aggregate signal. It should also be noted that substantial components of the LF data were in fact collected as individual weight data and converted to length using a common length-weight relationship. If the weight-length relationship shows significant regional heterogeneity, using region-specific relationships for such conversions outside of the stock assessment model may be a better approach.

The current models assume time-invariant selectivity for every fishery, and the results indicate that this may contribute materially to poor fit to the temporal structure of the LF data, even though the aggregate LF fit is acceptable. The assumption of time-invariant selectivity is a reasonable simplification for a first exploration (and one that is commonly made in many fisheries models), but it is a stronger assumption in a single-region "fleets-as-areas" context than in the spatial models, because selectivity here must simultaneously represent both gear “contact” selectivity and the potentially time-varying spatial availability of fish to each fishery. Allowing selectivity to vary through time, for example via time blocks, a smoothly time-varying spline or random effects, would likely improve the fit to the LF data and could reduce some of the regional and temporal residual patterns identified above. This would need to be balanced against the corresponding increase in the number of estimated parameters and the risk of increased confounding between time-varying selectivity and estimated recruitment, which cannot be as cleanly separated in a single-region model as they can where spatial parameters are also available to absorb some of that variability. There was some evidence of redundancy in the selectivity parameterisation for some fisheries, with a small number of estimated spline coefficients being close to their lower bound. This may be an area of potential simplification of the selectivity parameterisation that can at least partially offset the addition of temporal variability.

The CAAL results in particular again highlight the presence of regional heterogeneity in growth, which should be a high priority for the development of future integrated stock assessment models.

Final comment

Given the retrospective bias and data conflicts described above, we would stress that that stock status outcomes from these single-region models should be interpreted with caution and used only as a general cross-check against the spatial assessments rather than as a stand-alone basis for status determination. It is possible that the results indicate a more pessimistic picture of stock status than the spatial assessment models because a single-region model cannot recognise the fact that large portions of the WCPO outside of the equatorial areas have much lower levels of exploitation despite the fact that there seem to be substantial stocks in those very large but lightly exploited areas (e.g., on the basis of the spatial distribution of standardised CPUE, Teears et al., 2026). The single-region models, by their nature, are likely to be more indicative of exploitation conditions in the tropical areas, where the majority of the data originate.

References

Carvalho, F., Winker, H., Courtney, D., Kapur, M., Kell, L., Cardinale, M., Schirripa, M., Kitakado, T., Yemane, D., Piner, K. R., et al. et al. (2021). A cookbook for using model diagnostics in integrated stock assessments. *Fisheries Research*, 240, 105959. https://doi.org/10.1016/j.fishres.2021.105959.

Day, J, , A., Teears, T., Hampton, J., Davies, N., Castillo Jordán, C., Peatman, T., Scott, R., Scutt Phillips, J., McKechnie, S., Scott, F., Yao, N., Natandra, R., Pilling, G., Williams, P., and Hamer, P. (2023). Stock assessment of bigeye tuna in the western and central Pacific Ocean: 2023 (6Aug2023) – Final (Rev.02). WCPFC-SC19-SA-WP05. https://meetings.wcpfc.int/node/19353.

Ducharme-Barth, N., Vincent, M., Hampton, J., Hamer, P., Williams, P., and Pilling, G. (2020). *Stock assessment* of bigeye tuna in the western and central Pacific Ocean *(30July)-Rev.03*. WCPFC-SC16-SA-WP03. https://meetings.wcpfc.int/node/11693.

Ducharme-Barth, N., Webber, D., Neubauer, P., Kim, K., Magnusson, A., and Hamer, P. (2026). OPAL: the open population assessment library. WCPFC-SC22-2026-SA-WP02. https://meetings.wcpfc.int/node/32247.

Hamer, P. (2026). Summary Report from the SPC Pre-assessment Workshop – March 2026. WCPFC-SC22-2026-SA-IP01.

Hampton, J, and Fournier, D.A. (2001). A spatially-disaggregated, length-based, age-structured population model of yellowfin tuna (*Thunnus albacares*) in the western and central Pacific Ocean. Mar. Freshw. Res. 52:937−963.

Kim, K., et al. (2026). Stock assessment of bigeye tuna in the western and central Pacific Ocean: 2026. WCPFC-SC22-2026-SA-WP06.

Macdonald, J., et al. (2023). Project 90 update: Better data on fish weights and lengths for scientific analyses. WCPFC-SC19-2023-ST-IP04.

, A., et al. (2026). Stock assessment of yellowfin tuna in the western and central Pacific Ocean: 2026. WCPFC-SC22-2026-SA-WP05.

Maunder, M. N. and Piner, K. R. (2015). Contemporary fisheries stock assessment: many issues still remain. ICES Journal of Marine Science, 72(1):7–18.

Minte-Vera, C. V., Maunder, M. N., Aires-da Silva, A. M., Satoh, K., and Uosaki, K. (2017). Get the biology right, or use size-composition data at your own risk. Fisheries research, 192:114–125.

Mohn, R. (1999). The retrospective problem in sequential population analysis: an investigation using cod fishery and simulated data. *ICES Journal of Marine Science*, 56, 473-488. https://doi.org/10.1006/jmsc.1999.0481.

Peatman, T., Castillo–Jordán, C., Teears, T., , Kim, K., Hampton, J., and Hamer, P. 2026. Analysis of size frequency data for the 2026 bigeye and yellowfin assessments. WCPFC-SC22-2026-SA-IP06. https://meetings.wcpfc.int/node/32346.

Punt, A.E., Dunn, A., Elvarsson, B.P., Hampton, J., Hoyle, S.D., Maunder, M.N., Methot, R.D., and Nielsen, A. (2020). Essential features of the next-generation integrated fisheries stock assessment package: A perspective. Fisheries Research 229: 105617. https://doi.org/10.1016/j.fishres.2020.105617.

Teears, T., et al. (2026). Background Analyses and Data Inputs for the 2026 WCPO yellowfin and bigeye tuna stock assessment. WCPFC-SC22-2026-SA-IP03.

Declaration of generative AI and AI-assisted technologies in the SC paper preparation process

Claude AI (Sonnet 5) was used for final editing of the draft paper.

Acknowledgements

We are grateful to SPC-OFP colleagues for discussions and review of this paper. This work was supported by the WCPFC under the regular ‘scientific services’ and ‘additional resourcing SPC’ budget lines to the scientific services provider.

Table 1. Extraction and index fisheries defined for the single-region BIGEYE TUNA assessment model. Fishery definitions are identical to those used in the five-region 2026 bigeye tuna stock assessment (Kim et al., 2026). REGION refers to the region in which the fishery occurred (Figure 1a). Nationality: All – all flag states; AU – Australia; ID – Indonesia; JP – Japan; PH – Philippines; US – United States of America; VN - Vietnam.

FISHERY	GEAR	NATIONALITY	REGION
1. LL.WEST.1	Longline	All	1-WEST
2. LL.EAST.1	Longline	All	1-EAST
3. LL.US.1	Longline	US	1
4. LL.ALL.2	Longline	All	2
5. LL.OS.2	Longline	All offshore	2
6. LL.ARCH.3	Longline	All	3-ARCH
7. LL.WEST.3	Longline	All	3-WEST
8. LL.ALL.4	Longline	All	4
9. LL.OS.3	Longline	All offshore	3-WEST
10. LL.ALL.5	Longline	All	5
11. LL.AU.5	Longline	AU	5
12. PS.JP.1	Purse seine	JP	1
13. PL.JP.1	Pole-and-line	JP	1
14. HL.ID.2	Handline	ID	2
15. HL.PH.2	Handline	PH	2
16. PL.ALL.2	Pole-and-line	All	2
17. PS.ID.DOM2	Purse seine	ID	2
18. PS.PH.DOM2	Purse seine	PH	2
19. PS.ASS.2	Purse seine associated sets	All except ID, PH DOM	2
20. PS.UNA.2	Purse seine unassociated sets	All except ID, PH DOM	2
21. MISC.ID.2	Miscellaneous	ID	2
22. MISC.PH.2	Miscellaneous	PH	2
23. MISC.VN.2	Miscellaneous	VN	2
24. PL.ALL.3	Pole-and-line	All	3
25. PS.ASS.3	Purse seine associated sets	All	3
26. PS.ASS.4	Purse seine associated sets	All	4
27. PS.UNA.3	Purse seine unassociated sets	All	3
28. PS.UNA.4	Purse seine unassociated sets	All	4
29. INDEX.WCPO	Longline	All	WCPO

Table 2. Extraction and index fisheries defined for the single-region YELLOWFIN TUNA assessment model. Fishery definitions are identical to those used in the five-region 2026 yellowfin tuna stock assessment (Magnussen et al., 2026). REGION refers to the region in which the fishery occurred (Figure 1b). Nationality: All – all flag states; AU – Australia; ID – Indonesia; JP – Japan; PH – Philippines; US – United States of America; VN - Vietnam.

FISHERY	GEAR	FLAG	REGION
1. LL.WEST.1	Longline	All	1-WEST
2. LL.EAST.1	Longline	All	1-EAST
3. LL.US.1	Longline	US	1
4. LL.ALL.2	Longline	All	2
5. LL.OS.2	Longline	All offshore	2
6. LL.ALL.3	Longline	All	3
7. LL.WEST.4	Longline	All	4-WEST
8. LL.EAST.4	Longline	All	4-EAST
9. LL.OS.4	Longline	All offshore	4-WEST
10. LL.ALL.5	Longline	All	5
11. LL.AU.5	Longline	AU	5
12. PS.JP.1	Purse seine	JP	1
13. PL.JP.1	Pole-and-line	JP	1
14. HL.ID.2	Handline	ID	2
15. HL.PH.2	Handline	PH	2
16. PL.ALL.2	Pole-and-line	All	2
17. PS.ID.DOM.2	Purse seine	ID	2
18. PS.PH.DOM.2	Purse seine	PH	2
19. PS.ASS.2	Purse seine associated sets	All except ID, PH DOM	2
20. PS.UNA.2	Purse seine unassociated sets	All except ID, PH DOM	2
21. MISC.ID.2	Miscellaneous	ID	2
22. MISC.PH.2	Miscellaneous	PH	2
23. MISC.VN.2	Miscellaneous	VN	2
24. PL.ALL.3	Pole-and-line	All	3
25. PS.ASS.3	Purse seine associated sets	All	3
26. PS.UNA.3	Purse seine unassociated sets	All	3
27. PL.ALL.4	Pole and line	All	4
28. PS.ASS.WEST.4	Purse seine associated sets	All	4-WEST
29. PS.ASS.EAST.4	Purse seine associated sets	All	4-EAST
30. PS.UNA.WEST.4	Purse seine unassociated sets	All	4-WEST
31. PS.UNA.EAST.4	Purse seine unassociated sets	All	4-EAST
32. INDEX.WCPO	Longline	All	WCPO

Table 3. Selectivity (Sel) assumptions.

Fishery	BIGEYE TUNA			YELLOWFIN TUNA		
	Spline nodes	Sel=0 ≤ age class	Sel=0 ≥ age class	Spline nodes	Sel=0 ≤ age class	Sel=0 ≥ age class
1	5	2	NA	5	2	NA
2	5	2	NA	5	2	NA
3	5	2	NA	5	2	NA
4	5	2	NA	5	2	NA
5	5	2	NA	5	2	NA
6	5	2	NA	5	2	NA
7	5	2	NA	5	2	NA
8	5	2	NA	5	2	NA
9	5	2	NA	5	2	NA
10	5	2	NA	5	2	NA
11	5	2	NA	5	2	NA
12	8	2	25	6	NA	NA
13	8	1	30	6	NA	NA
14	5	NA	NA	5	5	NA
15	5	5	NA	5	5	NA
16	5	NA	25	5	NA	25
17	5	NA	25	5	NA	25
18	5	NA	25	5	NA	25
19	5	NA	25	5	NA	25
20	5	NA	NA	5	NA	NA
21	5	NA	10	5	NA	10
22	5	NA	7	5	NA	10
23	5	NA	6	5	NA	10
24	5	NA	25	5	NA	25
25	5	NA	25	5	NA	25
26	5	NA	25	5	NA	30
27	5	NA	30	5	NA	25
28	5	NA	NA	5	NA	NA
29	5	2	NA	5	NA	NA
30				5	NA	NA
31				5	NA	NA
32				5	NA	NA

Table 4. Mohn's ρ and terminal relative differences for bigeye tuna. Values are calculated from converged peels with finite terminal comparisons.

Quantity	Mohn's ρ	Mean terminal difference (%)	Terminal difference range (%)
Depletion	-0.354	-35.4	-42.5 to -28.6
Fishing mortality	0.888	88.8	36.8 to 222.7
Recruitment	-0.175	-17.5	-61.2 to 21.5
Spawning potential	-0.394	-39.4	-45.7 to -31.5

Table 5. Mohn's ρ and terminal relative differences for yellowfin tuna. Values are calculated from converged peels with finite terminal comparisons.

Quantity	Mohn's ρ	Mean terminal difference (%)	Terminal difference range (%)
Depletion	-0.217	-21.7	-33.9 to -12.1
Fishing mortality	0.325	32.5	-28.7 to 82.6
Recruitment	-0.037	-3.7	-43.0 to 58.6
Spawning potential	-0.351	-35.1	-51.8 to -22.0

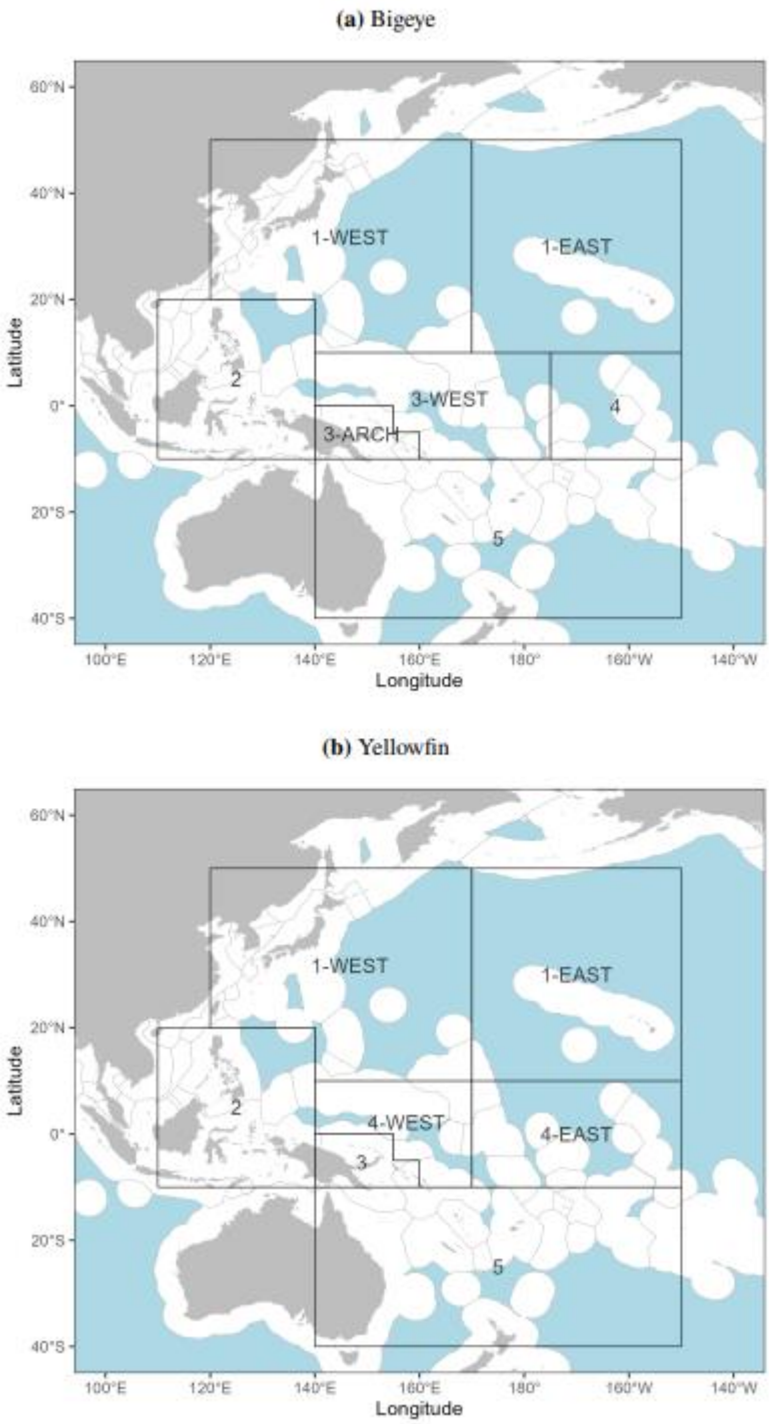

Figure 1. The spatial structures used to define fisheries for (a) bigeye and (b) yellowfin tuna.

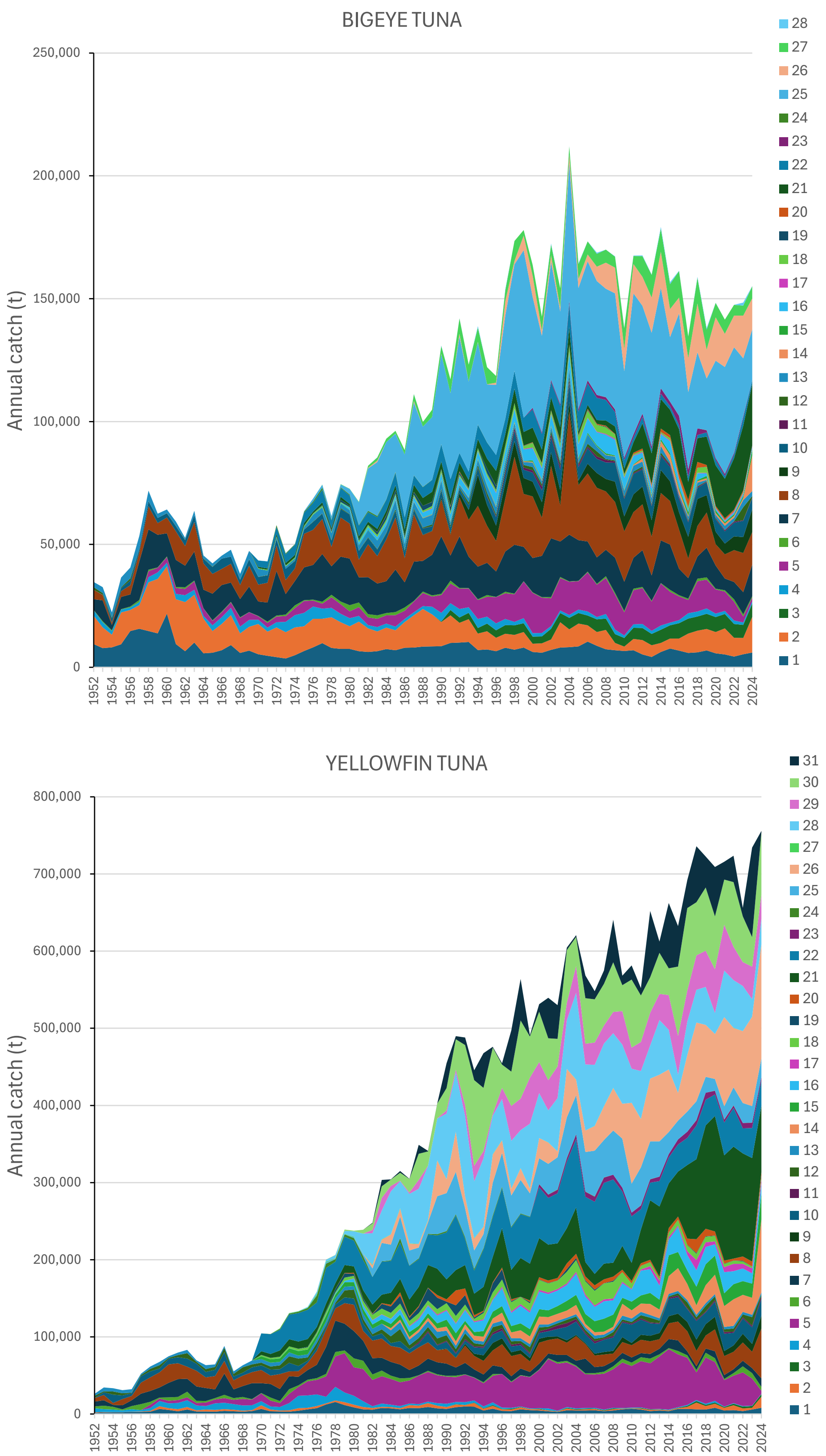

Figure 2. Annual catches by fisheries (see Table 1 and Table 2 for fishery descriptions) used in the WCPO models.

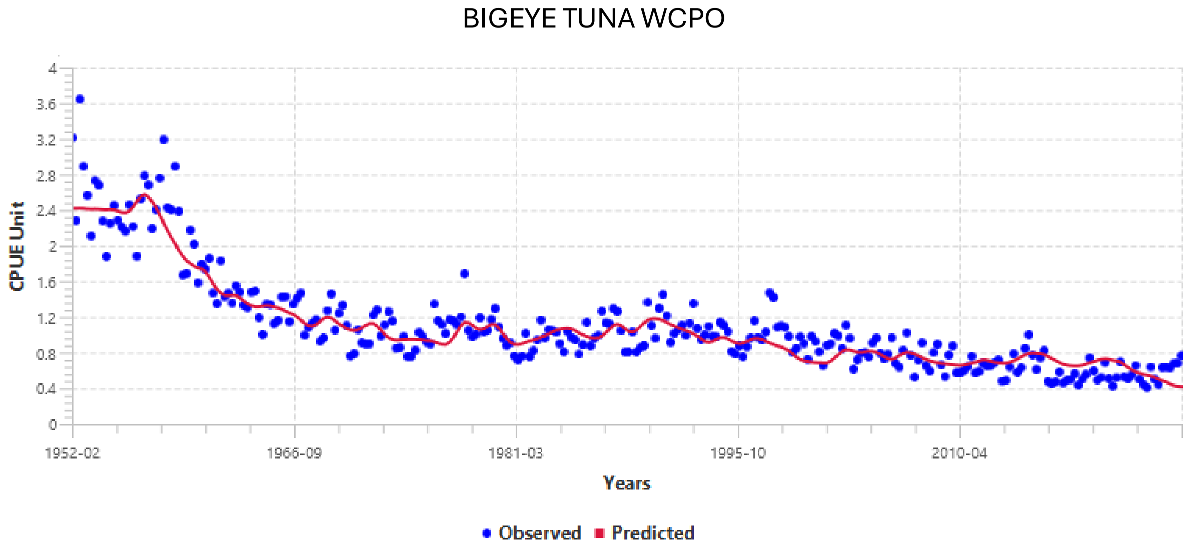

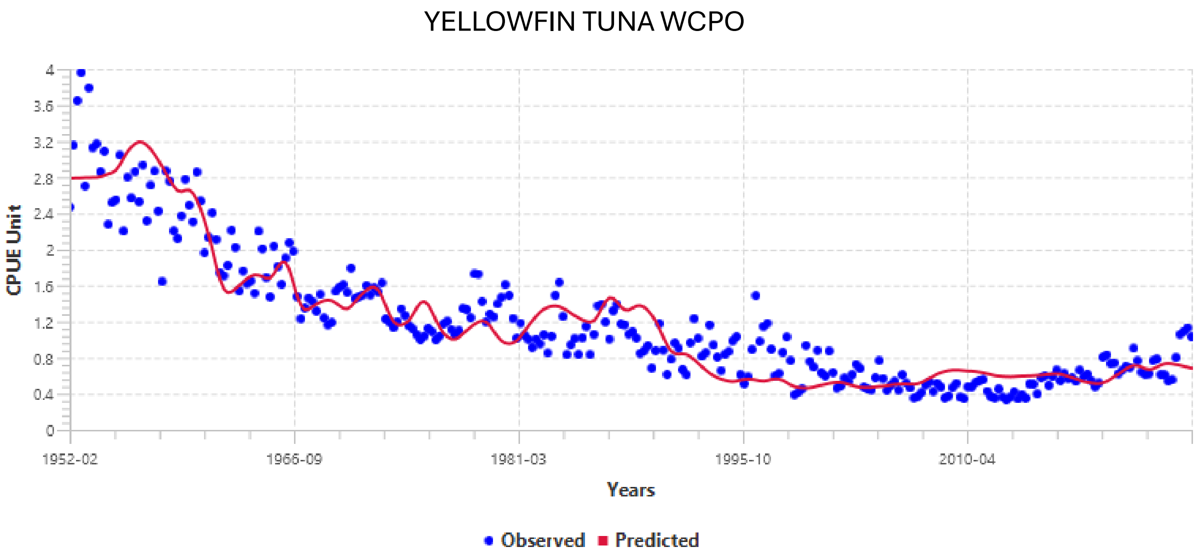

Figure 3. Fits to standardised catch-per-unit-effort for the bigeye and yellowfin tuna WCPO relative abundance indices.

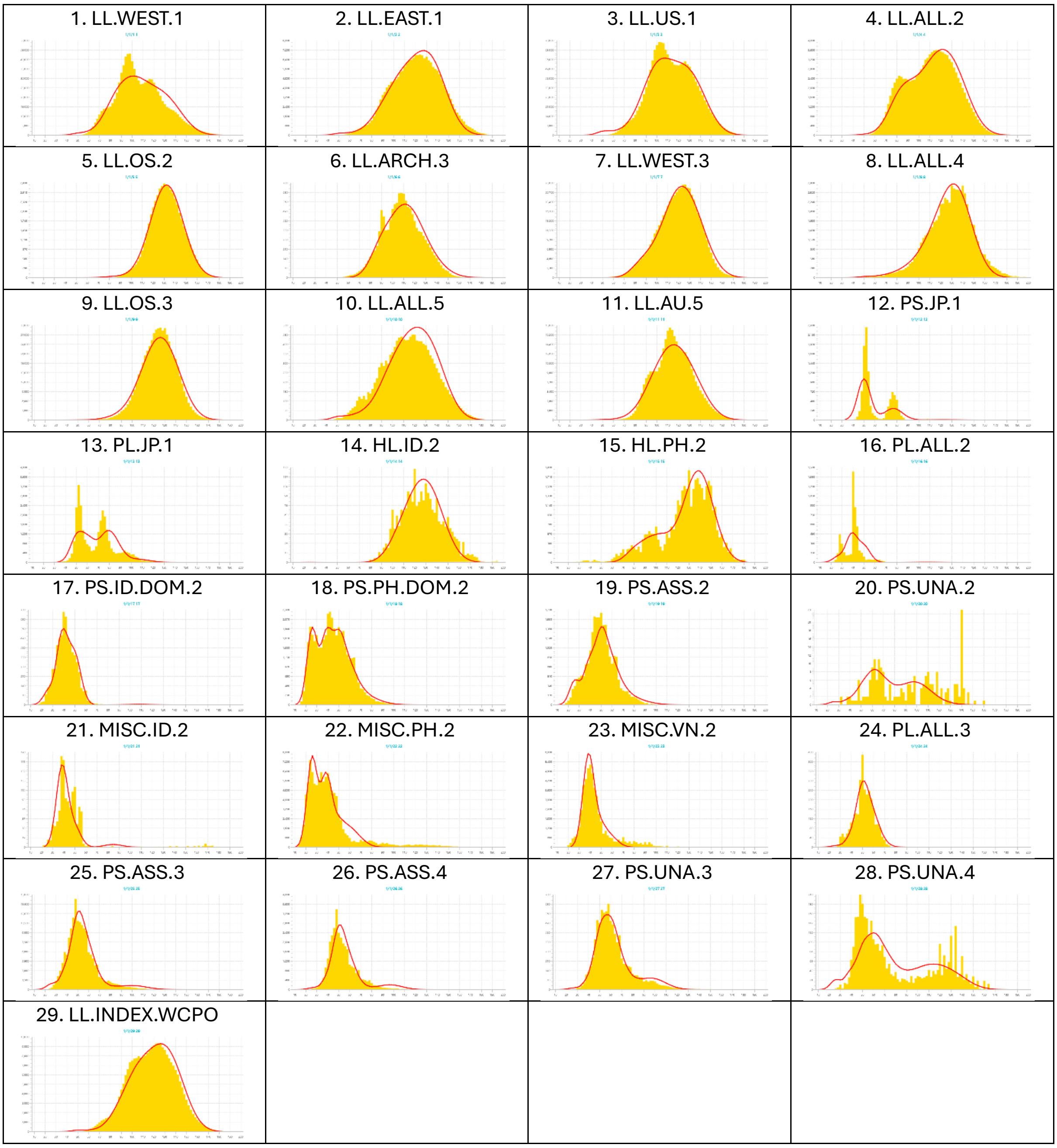

Figure 4. Fits (red lines) to time-aggregated size data (yellow histograms) for BIGEYE TUNA. Fishery names are described in Table 1.

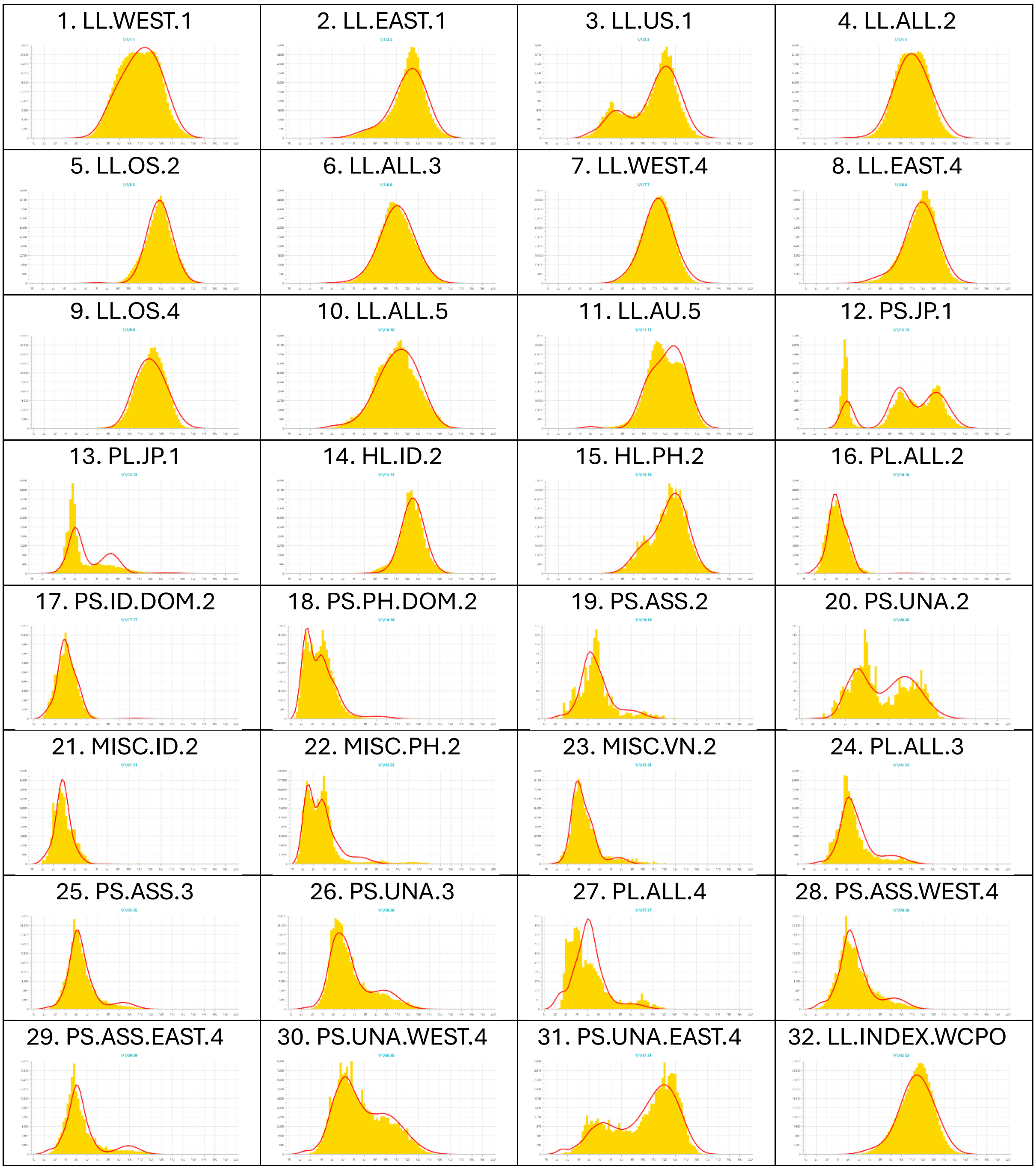

Figure 5. Fits (red lines) to time-aggregated size data (yellow histograms) for YELLOWFIN TUNA. Fishery names are described in Table 2.

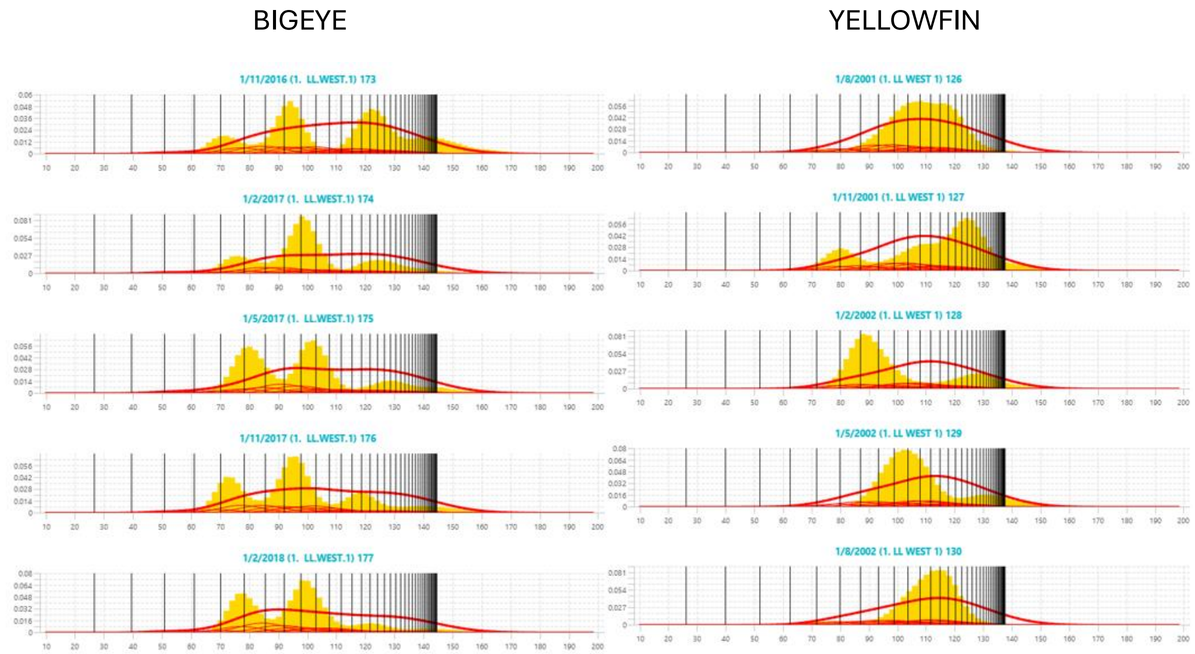

Figure 6. Examples of model fits (red lines) to quarterly length-frequency observations (yellow histograms) for Fishery 1 (LL.WEST.1) for bigeye and yellowfin tuna. The vertical bars in the plots indicate the sizes of estimated mean lengths for each age-class.

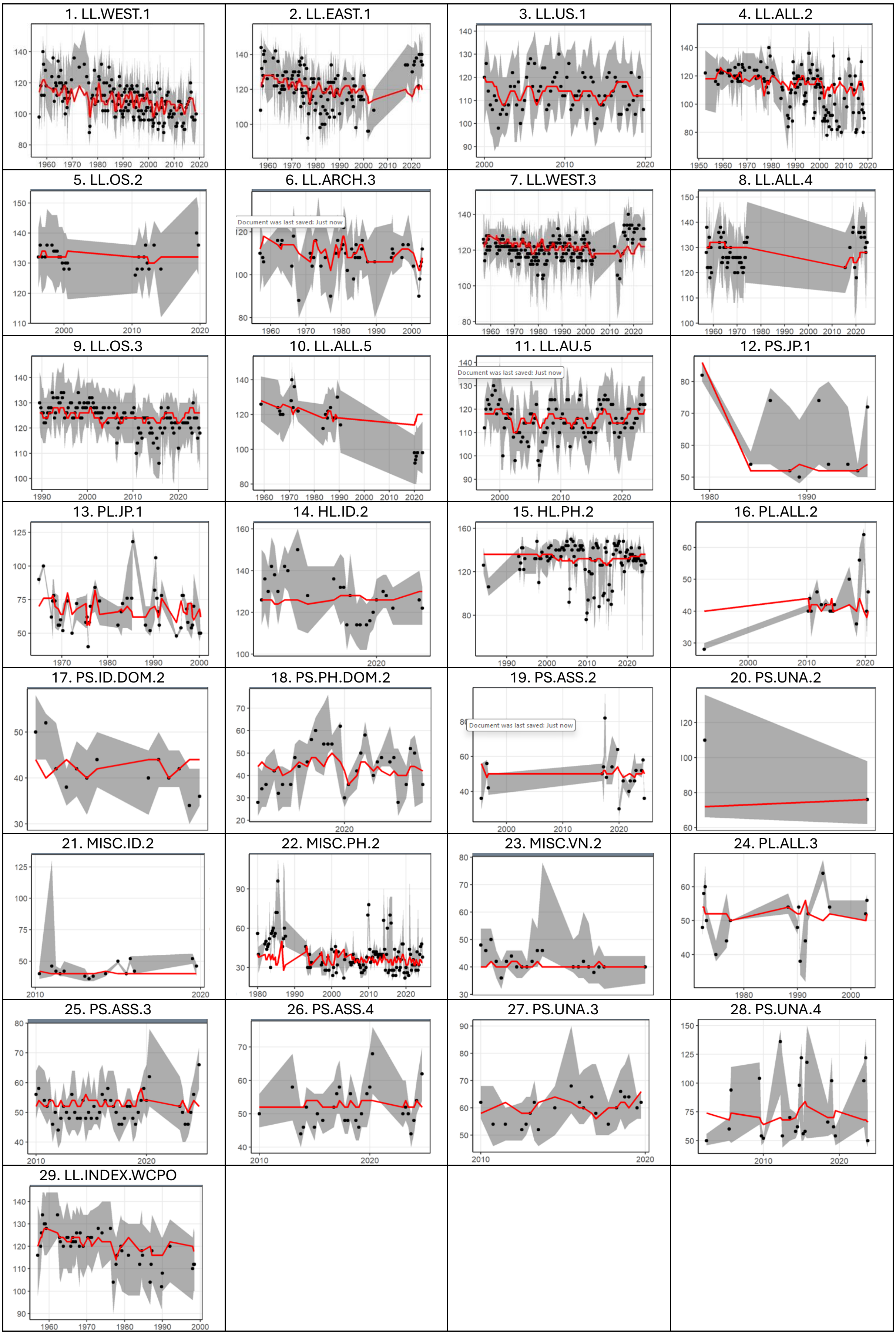

Figure 7. BIGEYE TUNA model estimated (lines) and observed (dots) median lengths with 95 percentiles (grey).

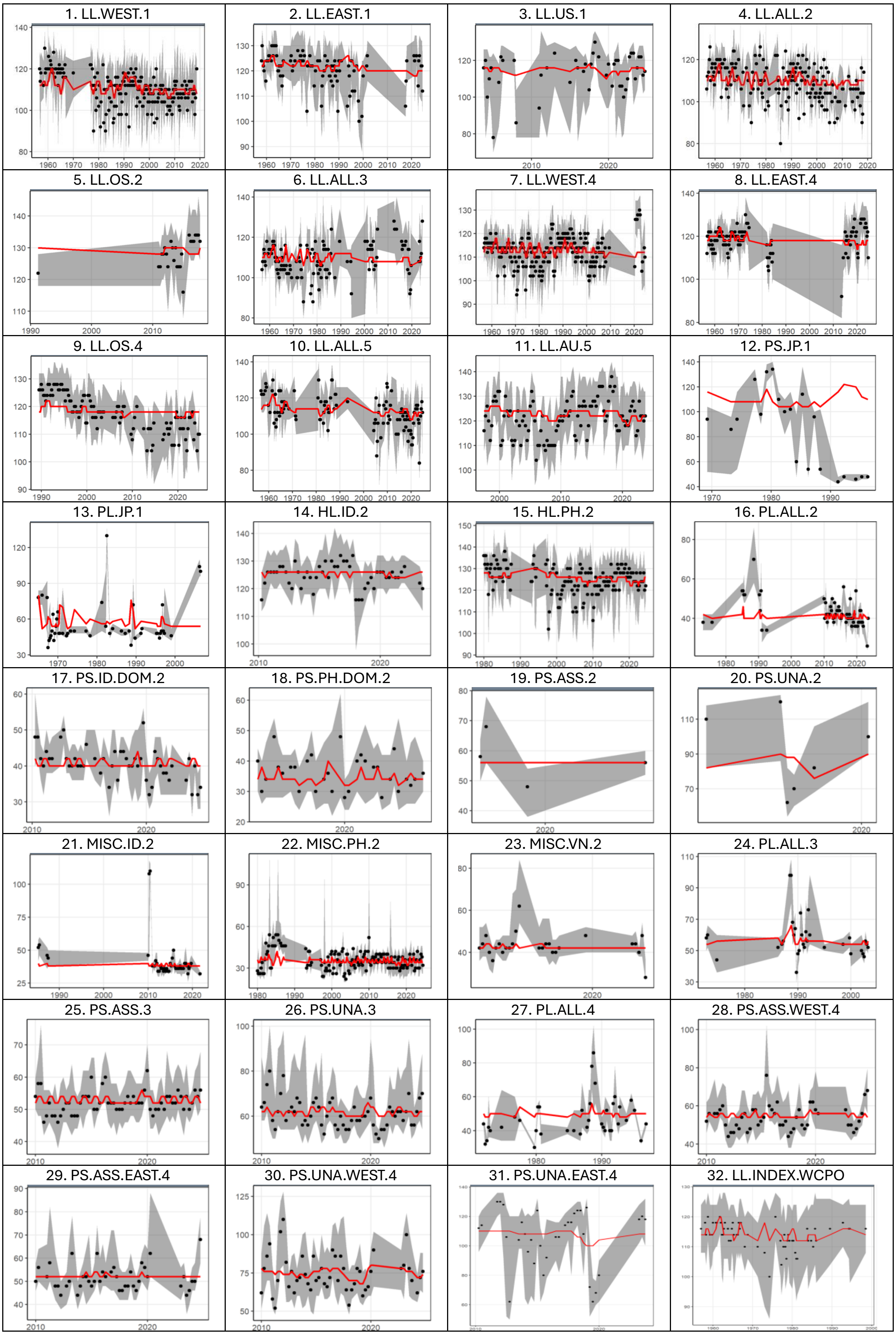

Figure 8. YELLOWFIN TUNA model estimated (lines) and observed (dots) median lengths with 95 percentiles (grey).

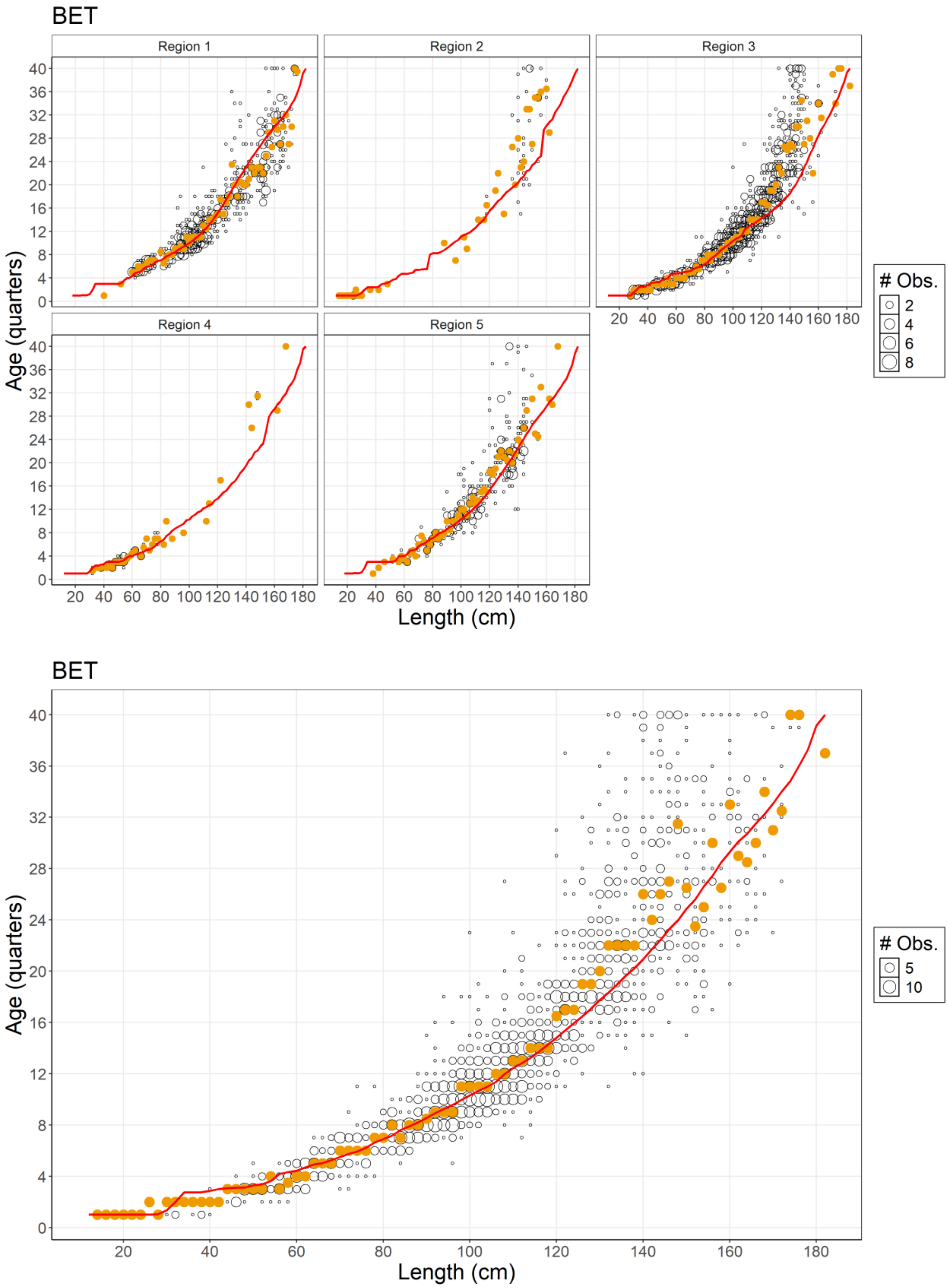

Figure 9. Fits to BIGEYE TUNA conditional-age-at-length data for samples aggregated by region (upper panels) and overall (lower panel). The open circles are the age-length observations; the solid orange circles are the medians of the observed ages for each 2-cm length bin; and the red line is the median of the predicted ages for each 2-cm length bin.

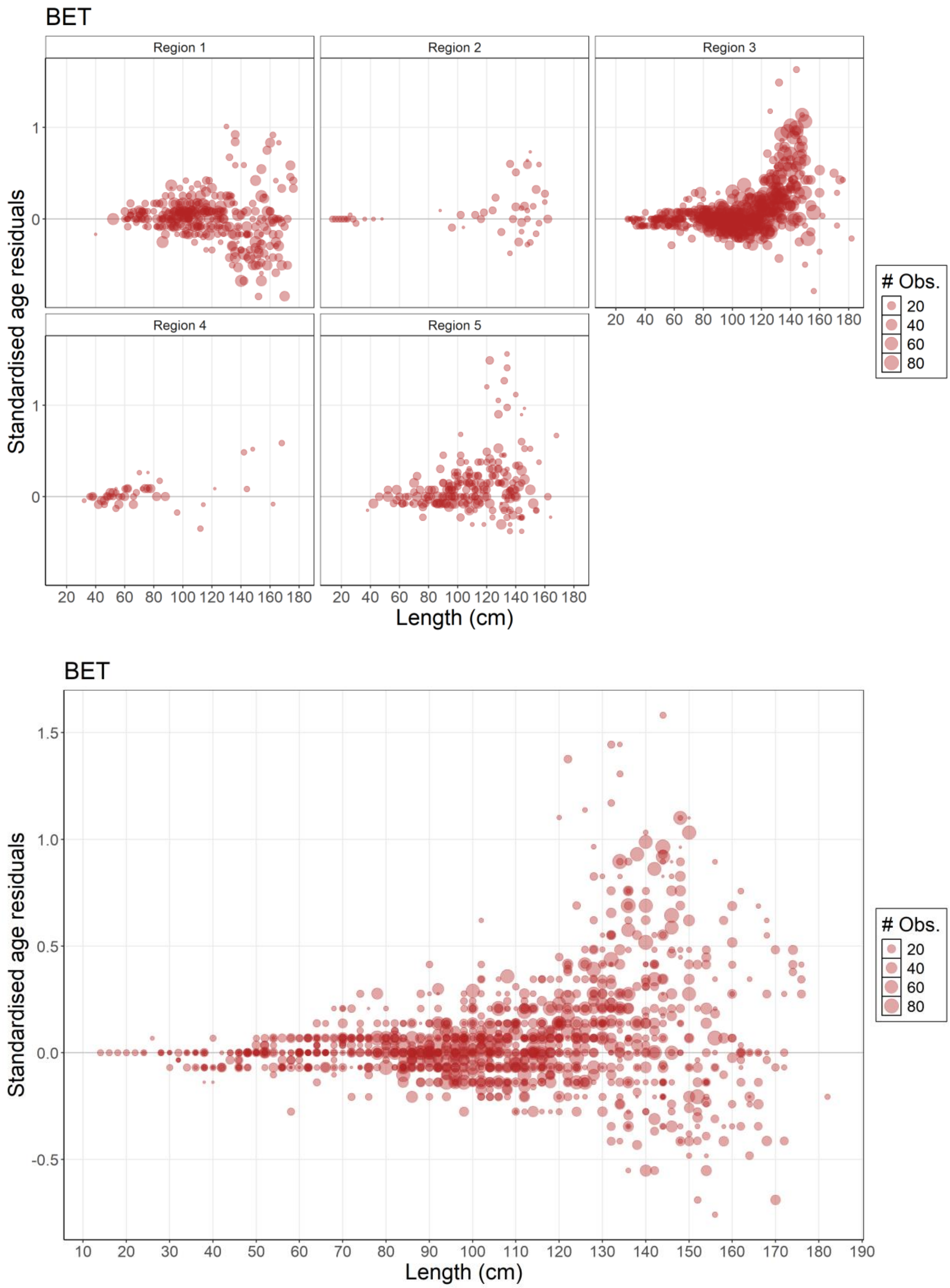

Figure 10. Standardised residuals of conditional age-at-length for BIGEYE TUNA for data aggregated by region (upper panels) and overall (lower panel).

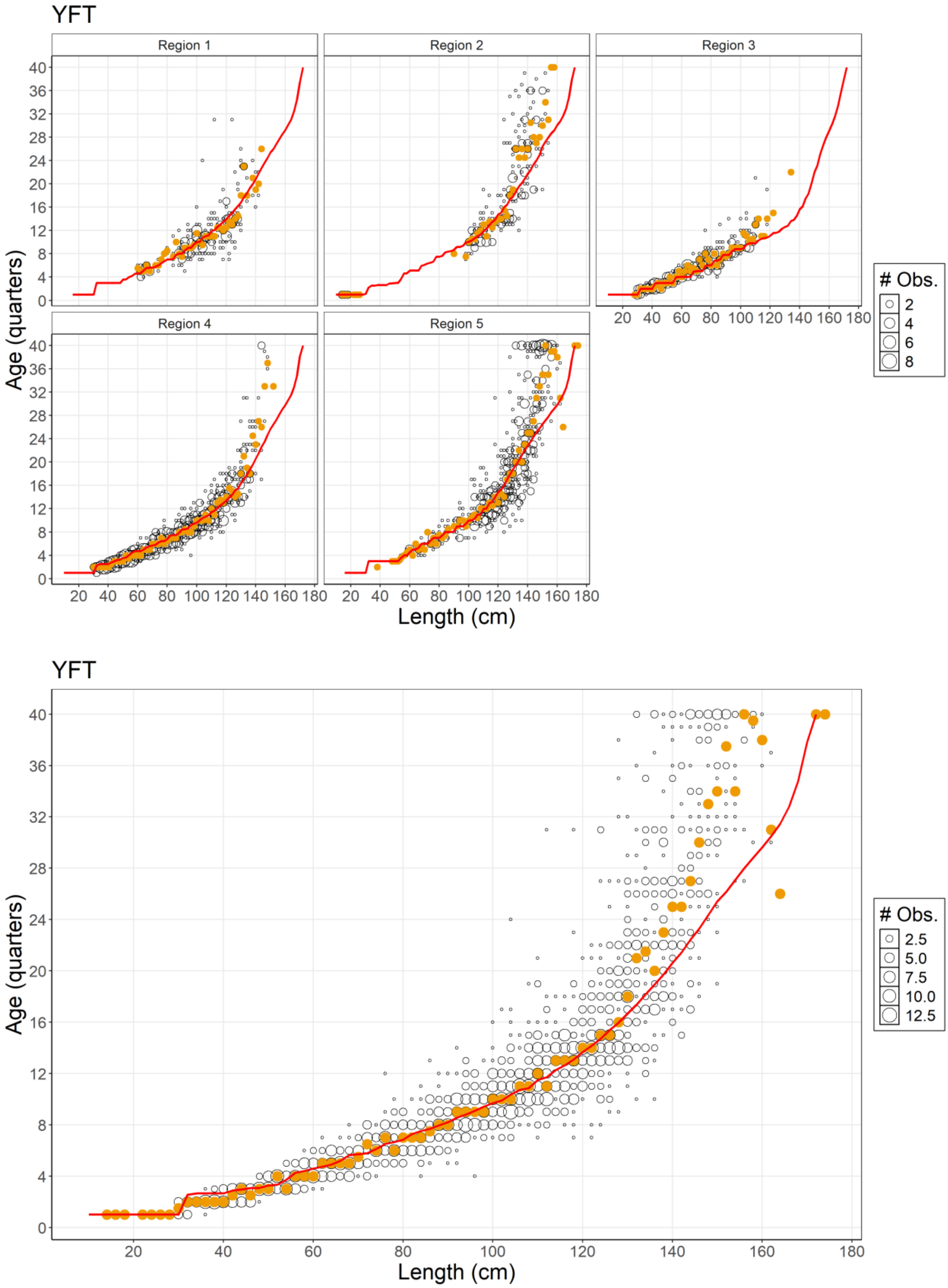

Figure 11. Fits to YELLOWFIN TUNA conditional-age-at-length data for samples aggregated by region (upper panels) and overall (lower panel). The open circles are the age-length observations; the solid orange circles are the medians of the observed ages for each 2-cm length bin; and the red line is the median of the predicted ages for each 2-cm length bin.

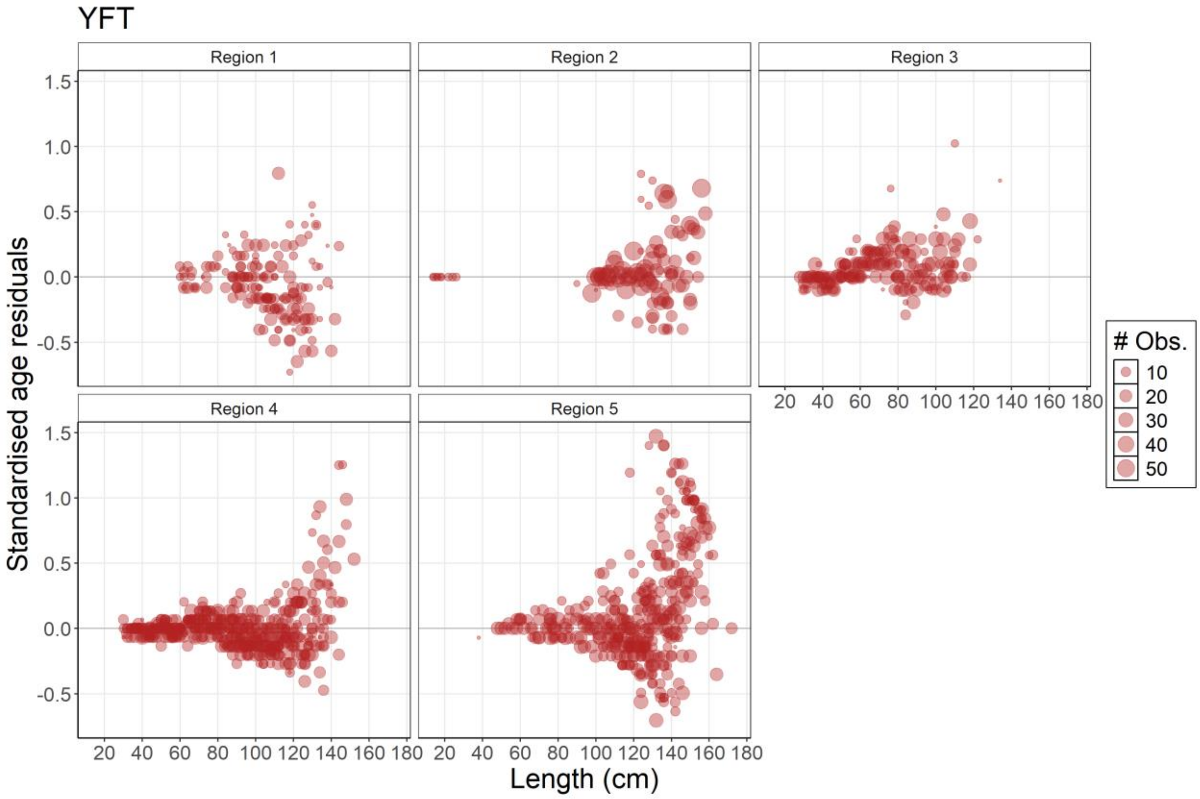

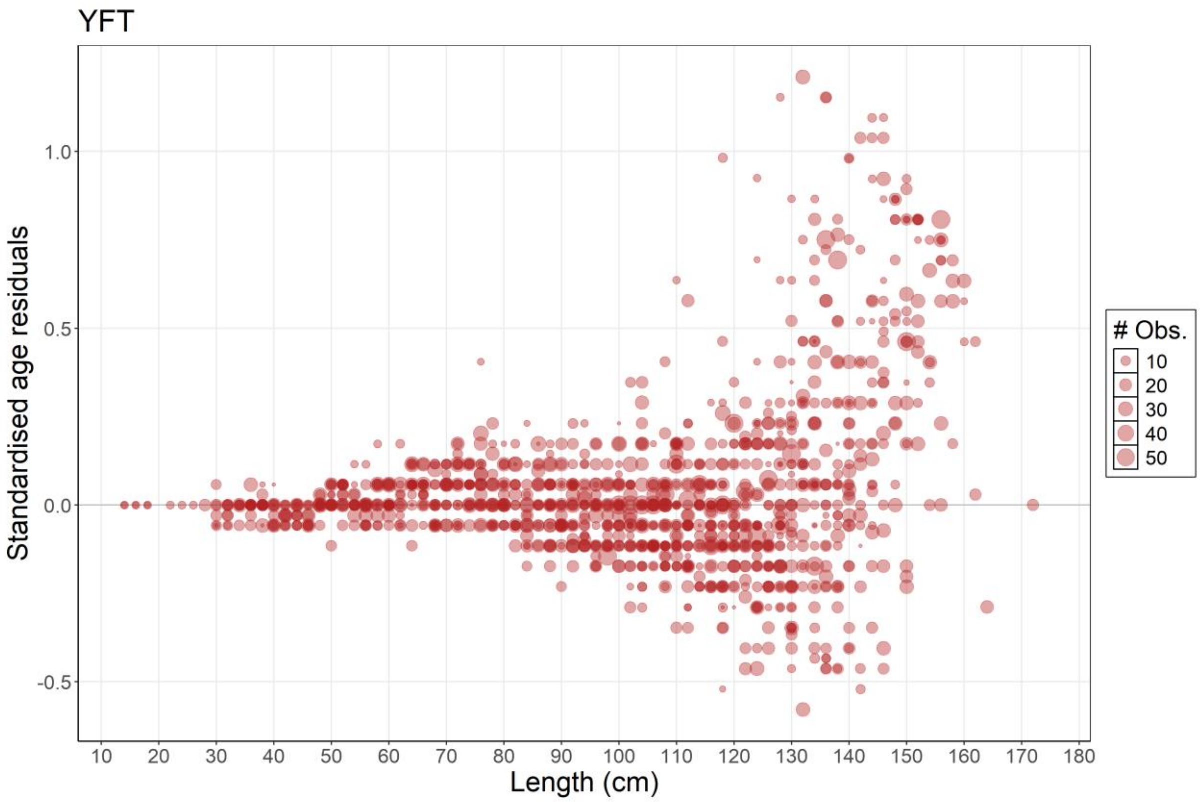

Figure 12. Standardised residuals of conditional age-at-length for YELLOWFIN TUNA for data aggregated by region (upper panels) and overall (lower panel).

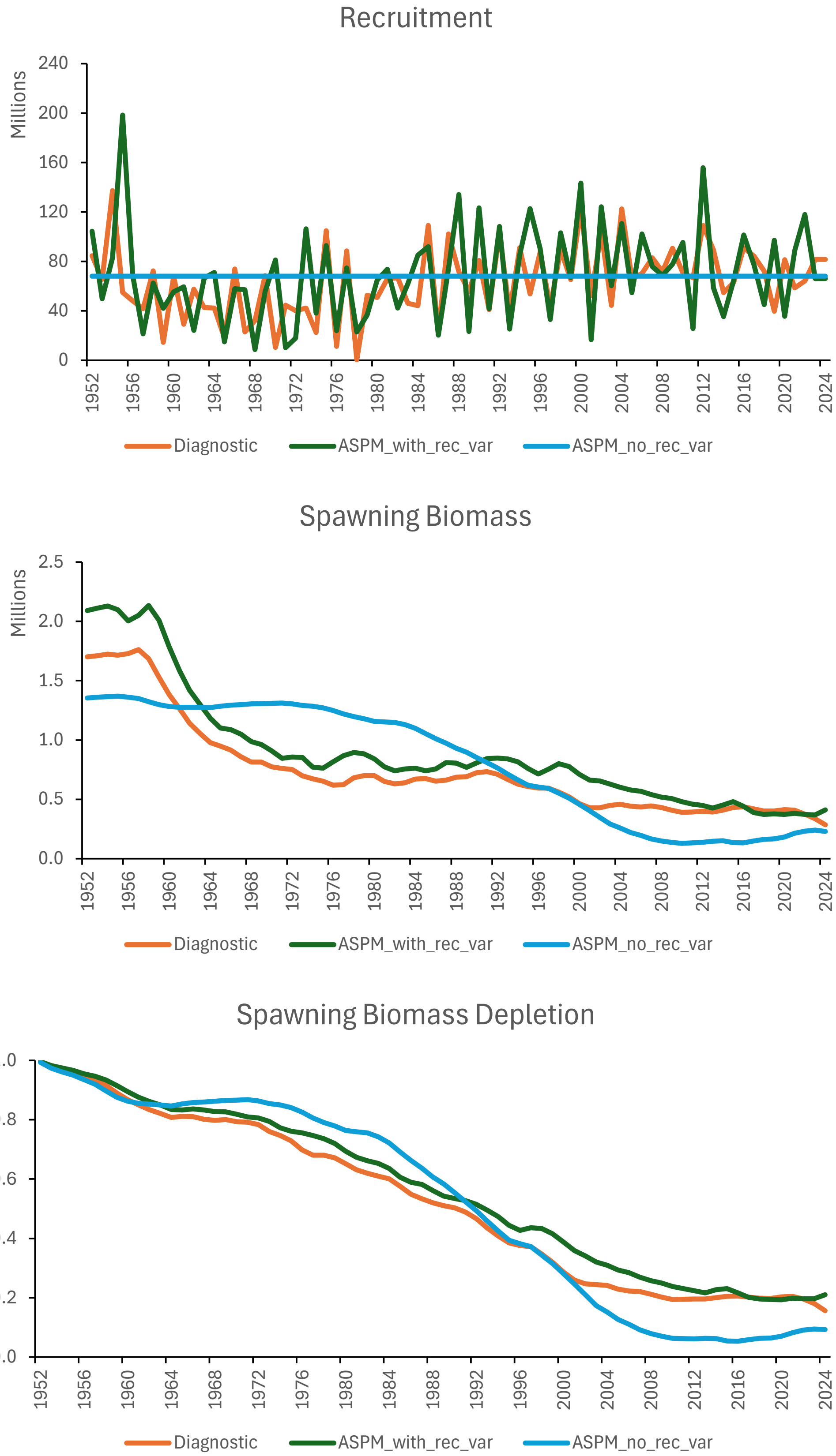

Figure 13. Results of age-structured production model (ASPM) analysis for BIGEYE TUNA with and without recruitment variability, compared to the single region model (Diagnostic).

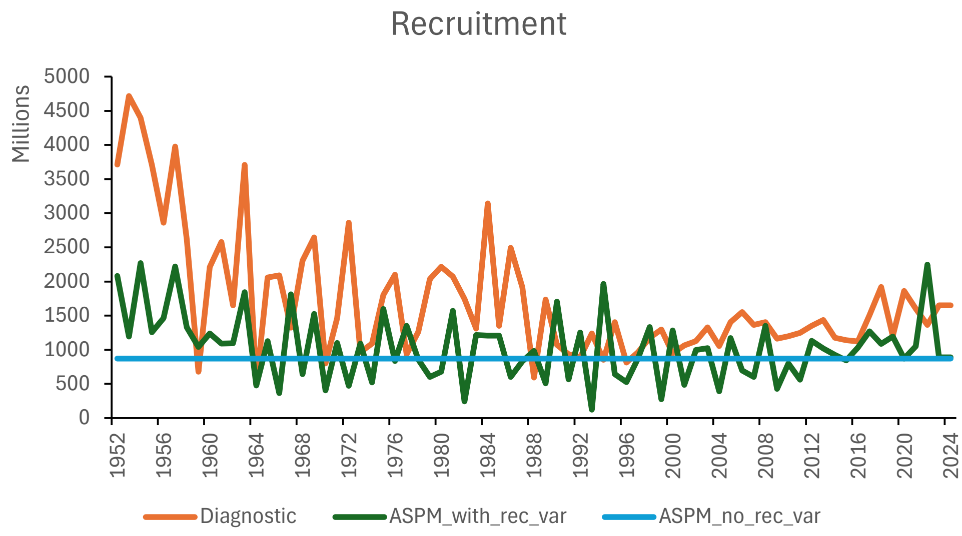

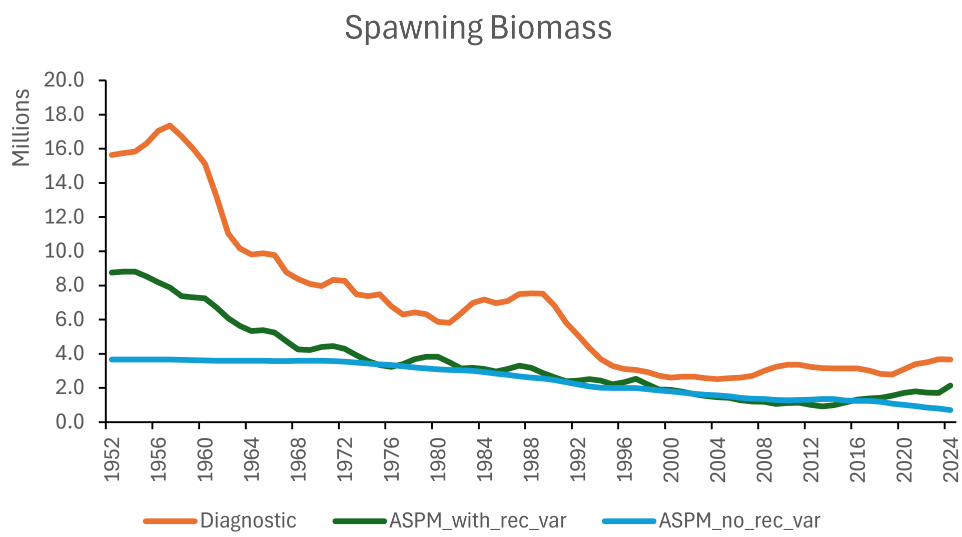

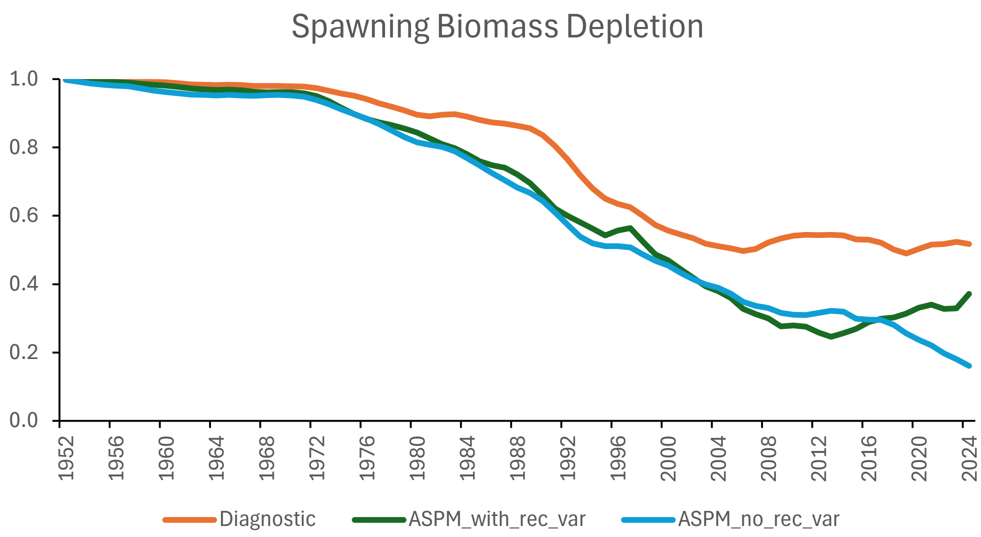

Figure 14. Results of age-structured production model (ASPM) analysis for YELLOWFIN TUNA with and without recruitment variability, compared to the single region model (Diagnostic).

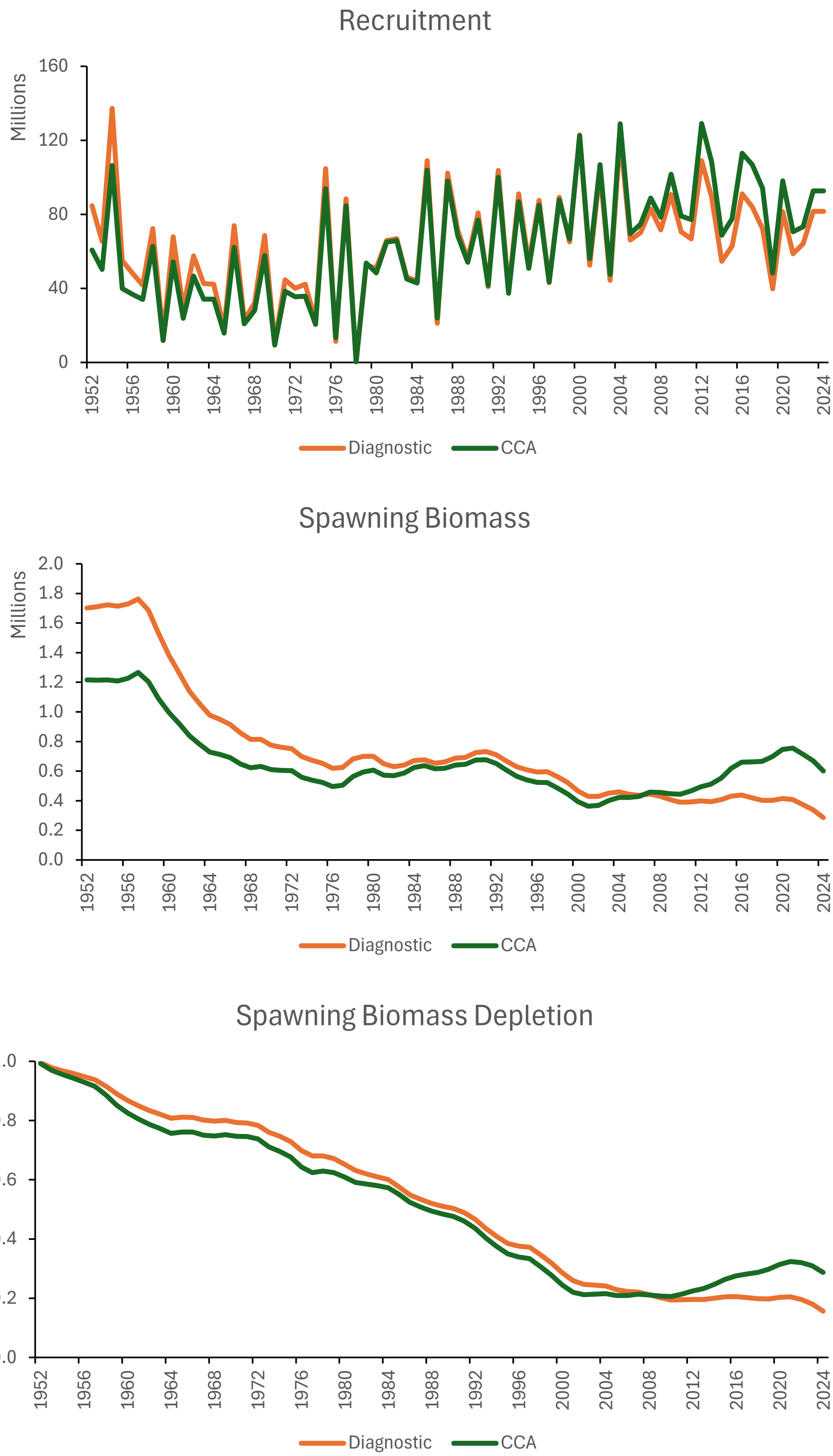

Figure 15. Results of catch-curve analysis ((CCA)) analysis for BIGEYE TUNA, compared to the single region model (Diagnostic).

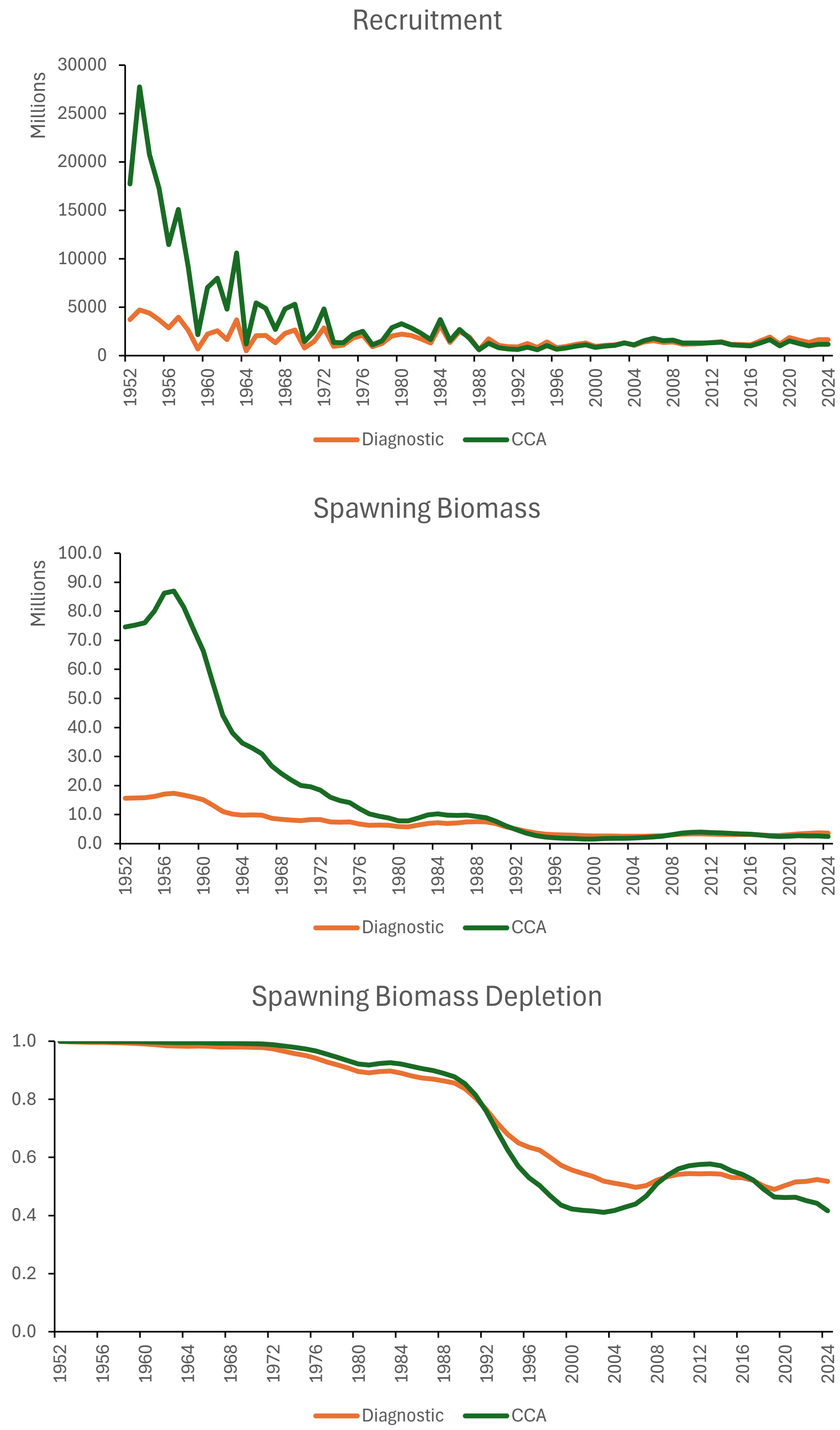

Figure 16. Results of catch-curve analysis ((CCA)) analysis for YELLOWFIN TUNA, compared to the single region model (Diagnostic).

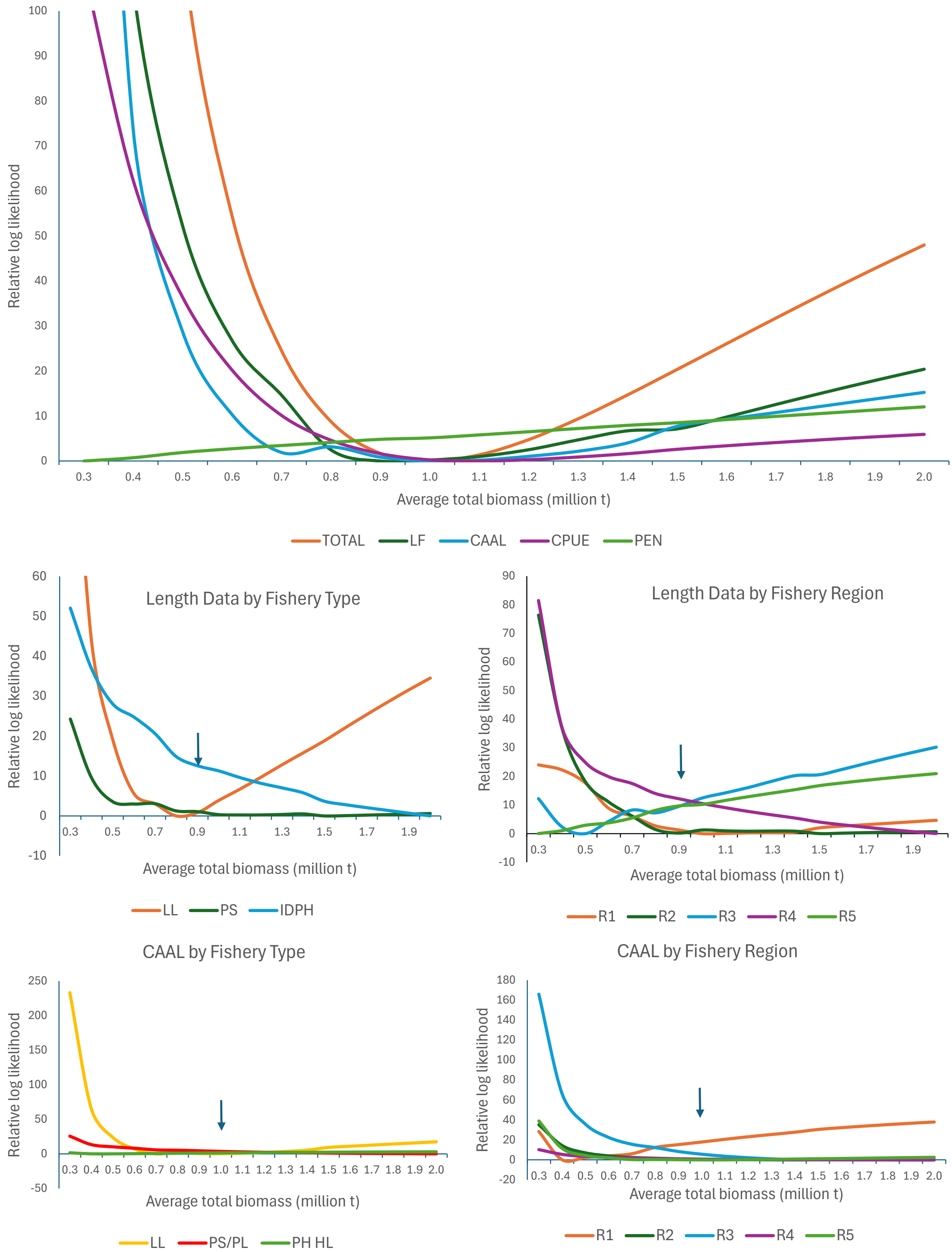

Figure 17. Likelihood profiles for the BIGEYE TUNA model. Upper panel – total likelihood by data type; middle panel – length data likelihood by fishery type and by fishery region; lower panel – conditional age-at-length (CAAL) data by fishery type and by fishery region.

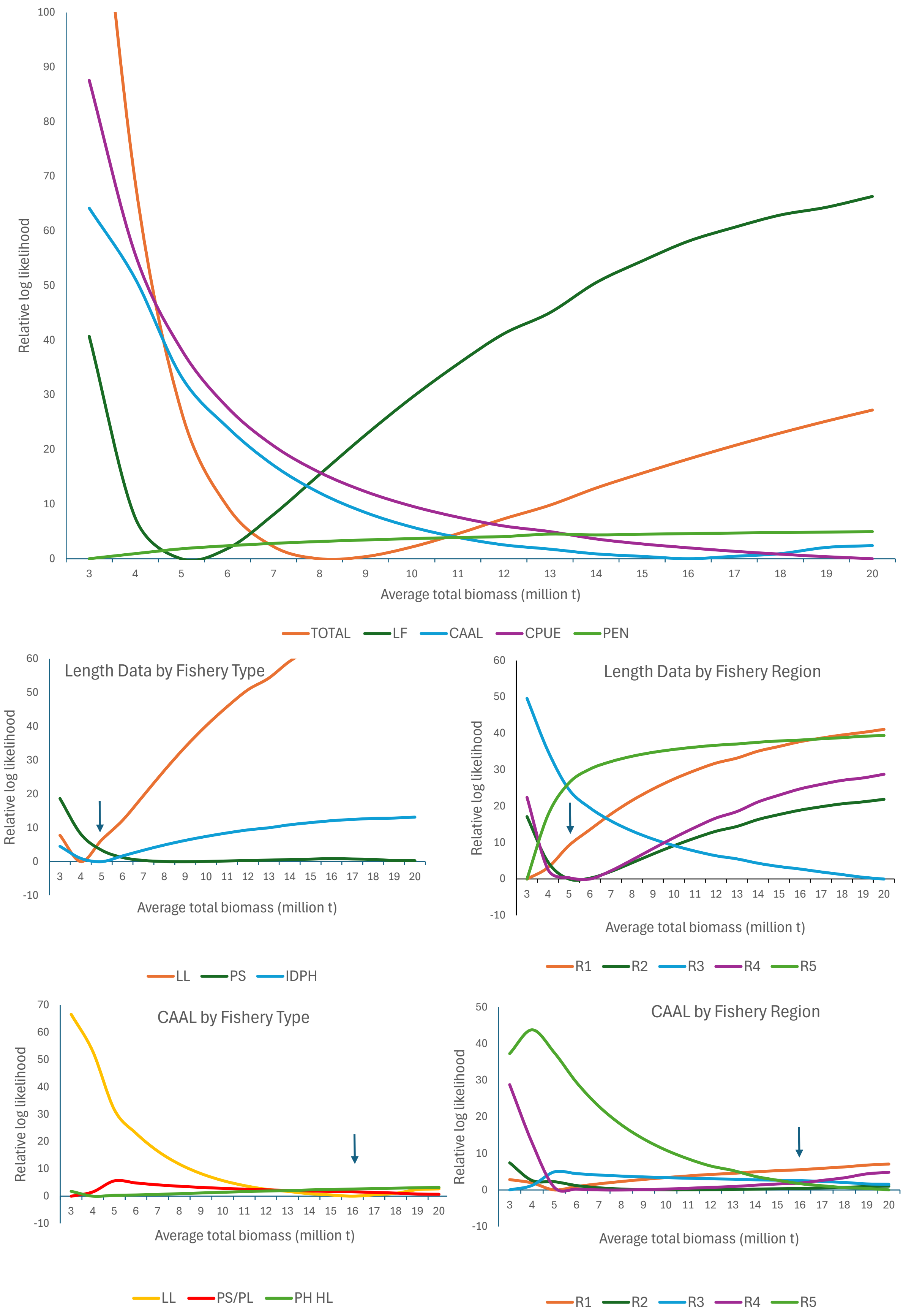

Figure 18. Likelihood profiles for the YELLOWFIN TUNA model. Upper panel – total likelihood by data type; middle panel – length data likelihood by fishery type and by fishery region; lower panel – conditional age-at-length (CAAL) data by fishery type and by fishery region. The arrows indicate the minimum for each data type.

BET

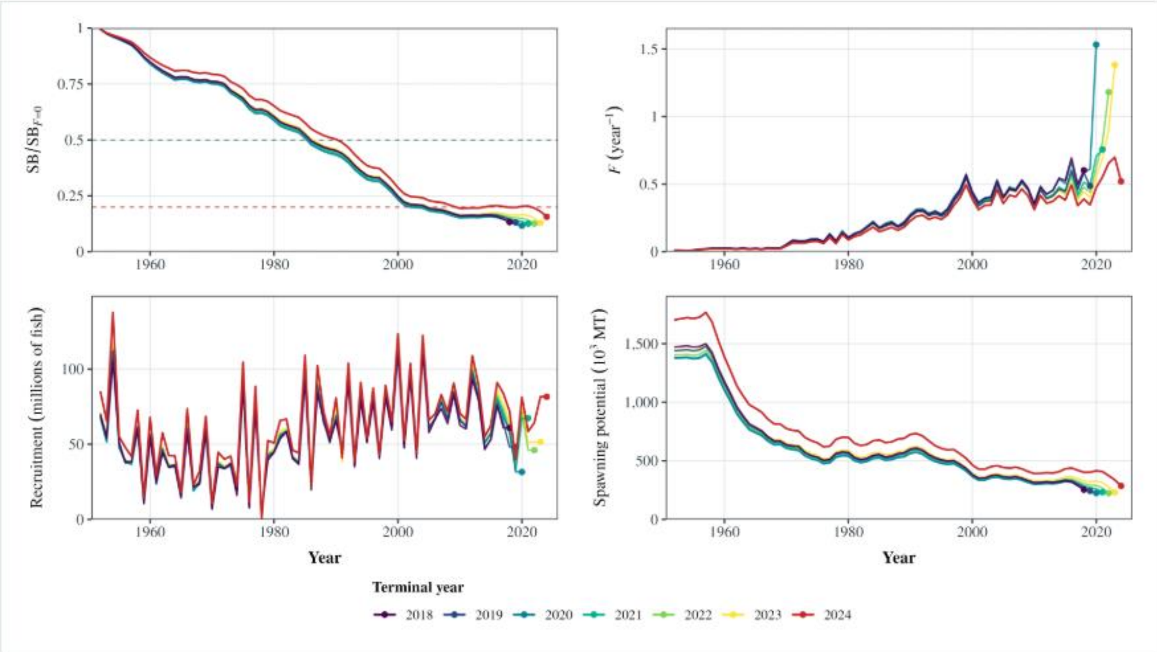

YFT

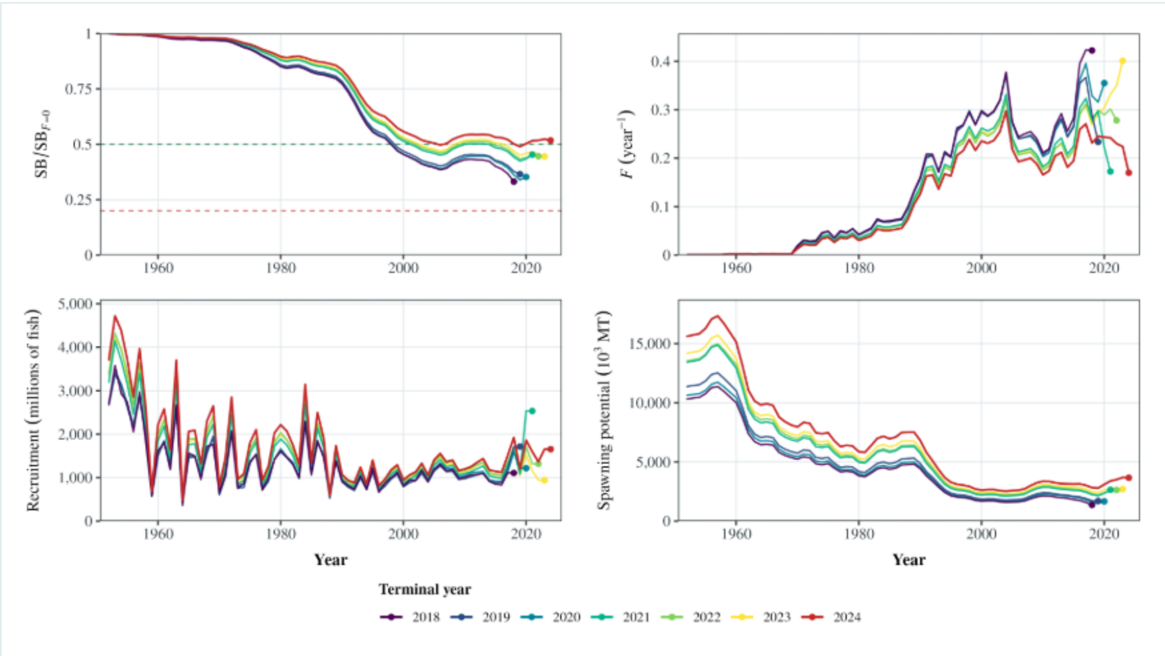

Figure 19. Retrospective analyses of the bigeye (upper panels) and yellowfin (lower panels) tuna single-region models. The quantities plotted for each model are (L to R, top to bottom) SB depletion, annual fishing mortality, and recruitment.

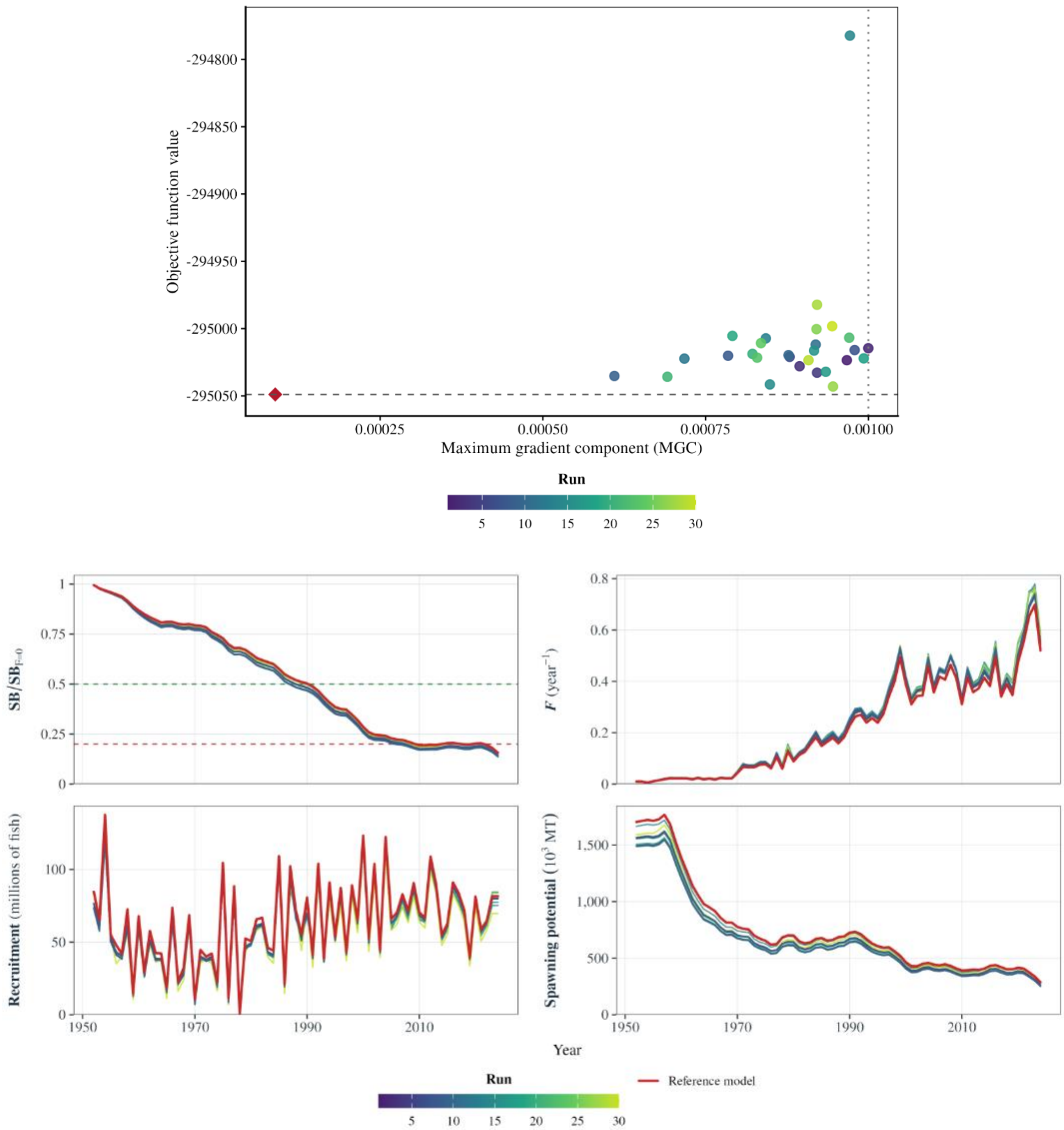

Figure 20. Jitter analysis of the BIGEYE tuna single-region model. The top panel shows the objective function values of the jittered models (blue-green dots) and that of the reference model (red diamond). The quantities plotted in the lower panel (L to right, top to bottom) are SB depletion, annual fishing mortality, recruitment and SB.

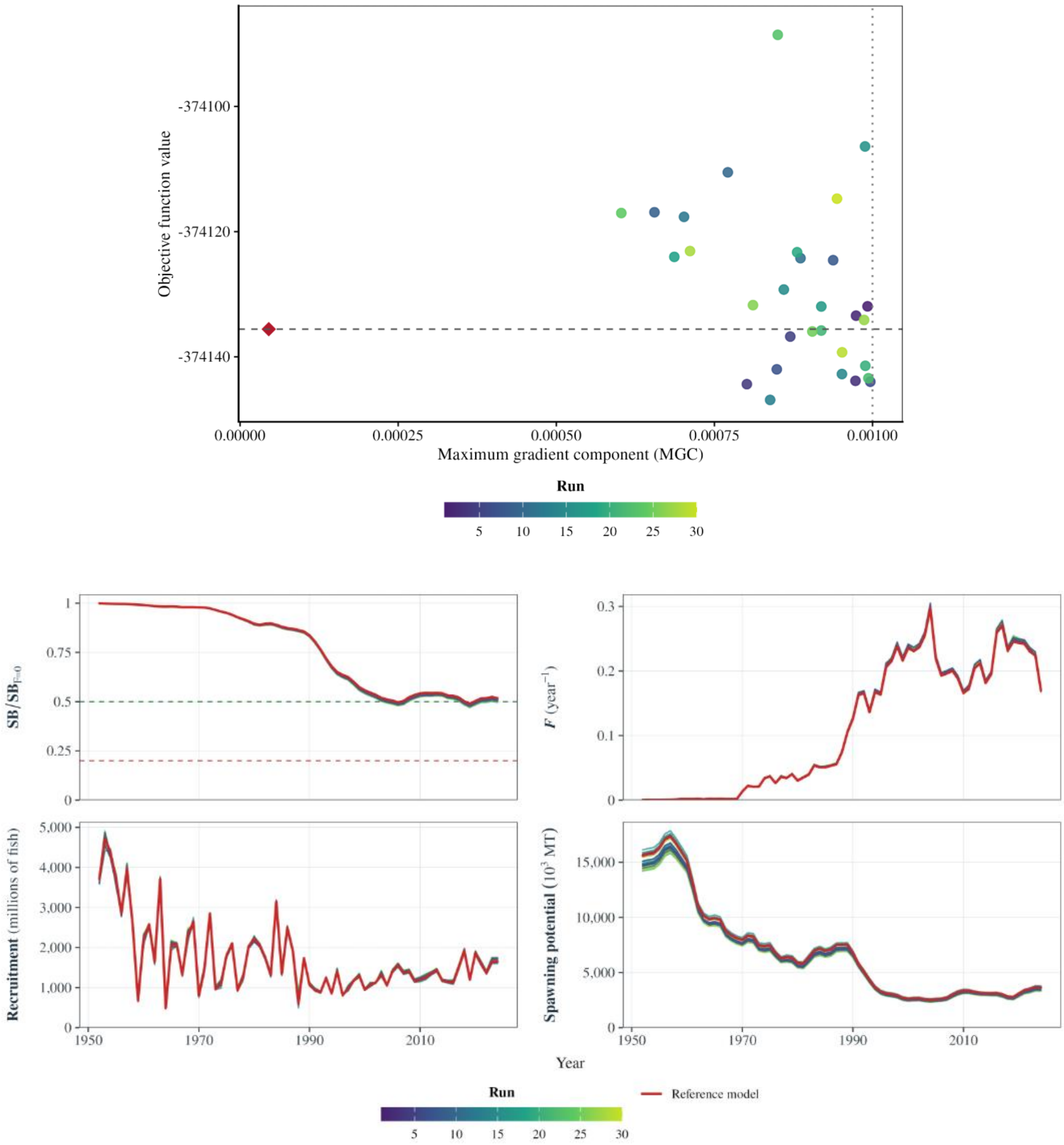

Figure 21. Jitter analysis of the YELLOWFIN tuna single-region model. The top panel shows the objective function values of the jittered models (blue-green dots) and that of the reference model (red diamond). The quantities plotted in the lower panel (L to right, top to bottom) are SB depletion, annual fishing mortality, recruitment and SB.

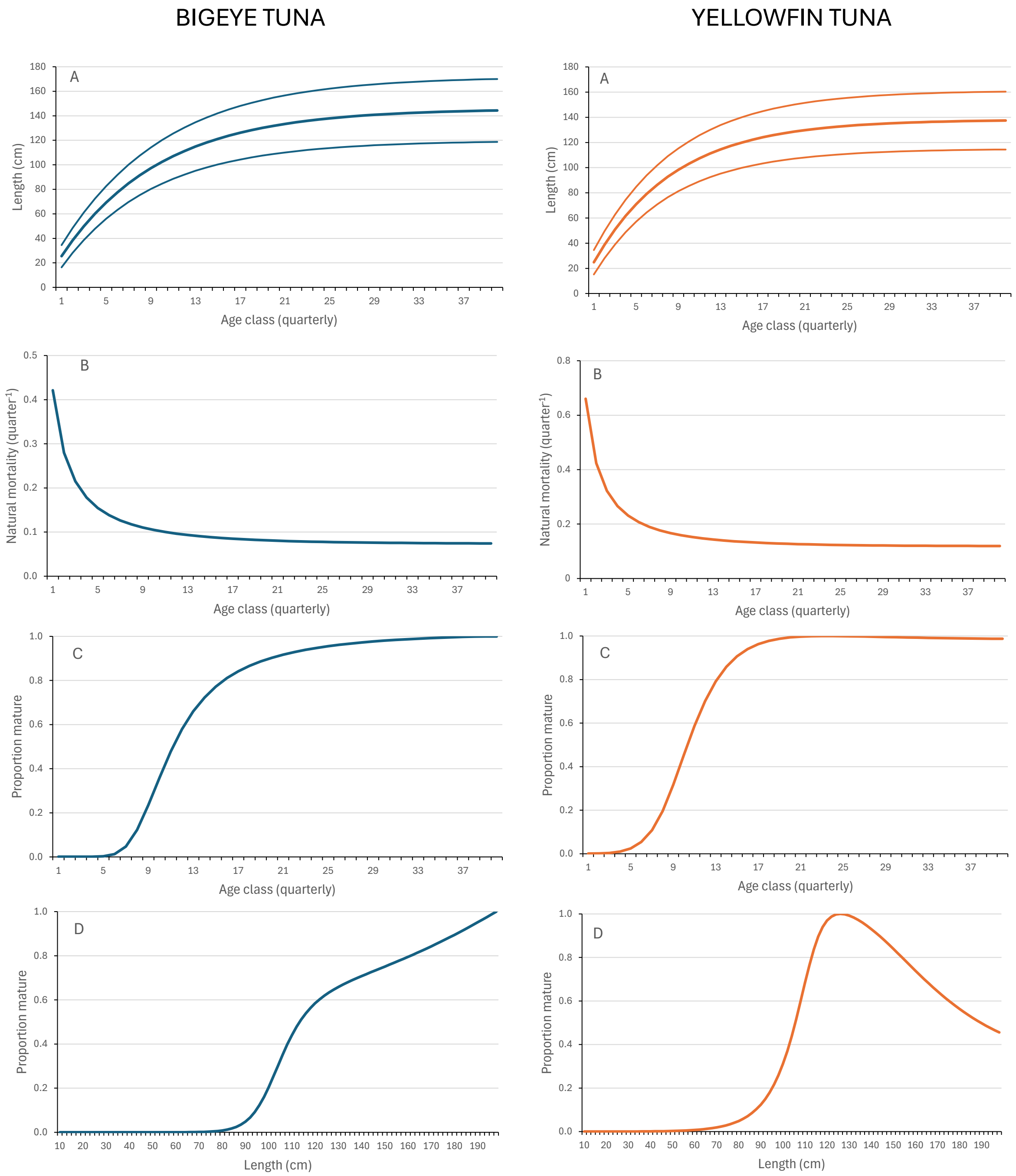

Figure 22. Estimated growth curve +/- 2 standard deviations of estimated length-at-age (A), natural mortality (B), maturity-at-age (C) and the input maturity-at-length (D) for BIGEYE TUNA (left) and YELLOWFIN TUNA (right).

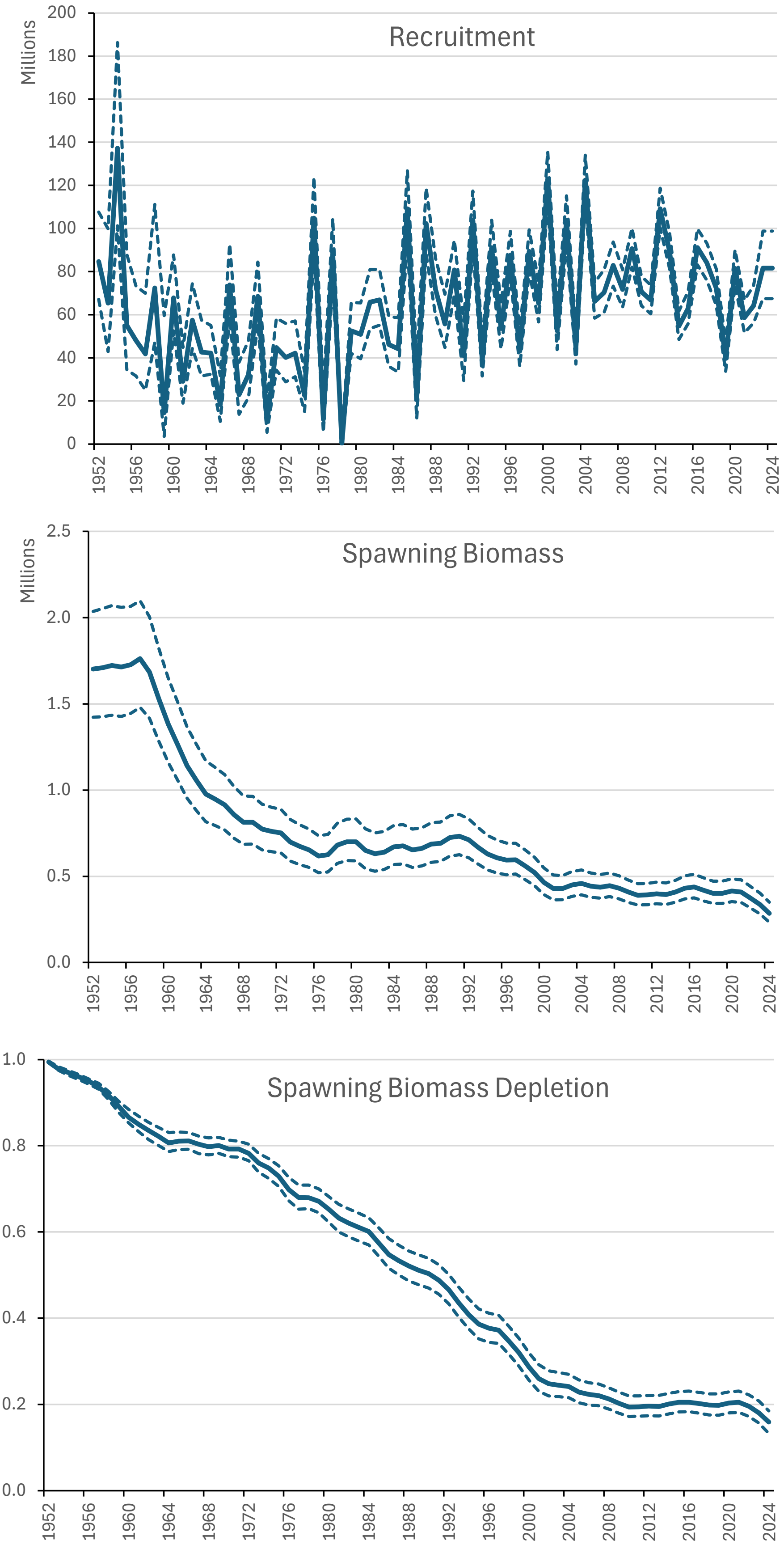

Figure 23. Estimated recruitment, spawning biomass and spawning biomass depletion (solid lines) and estimated 95% confidence intervals (dashed lines) for BIGEYE TUNA.

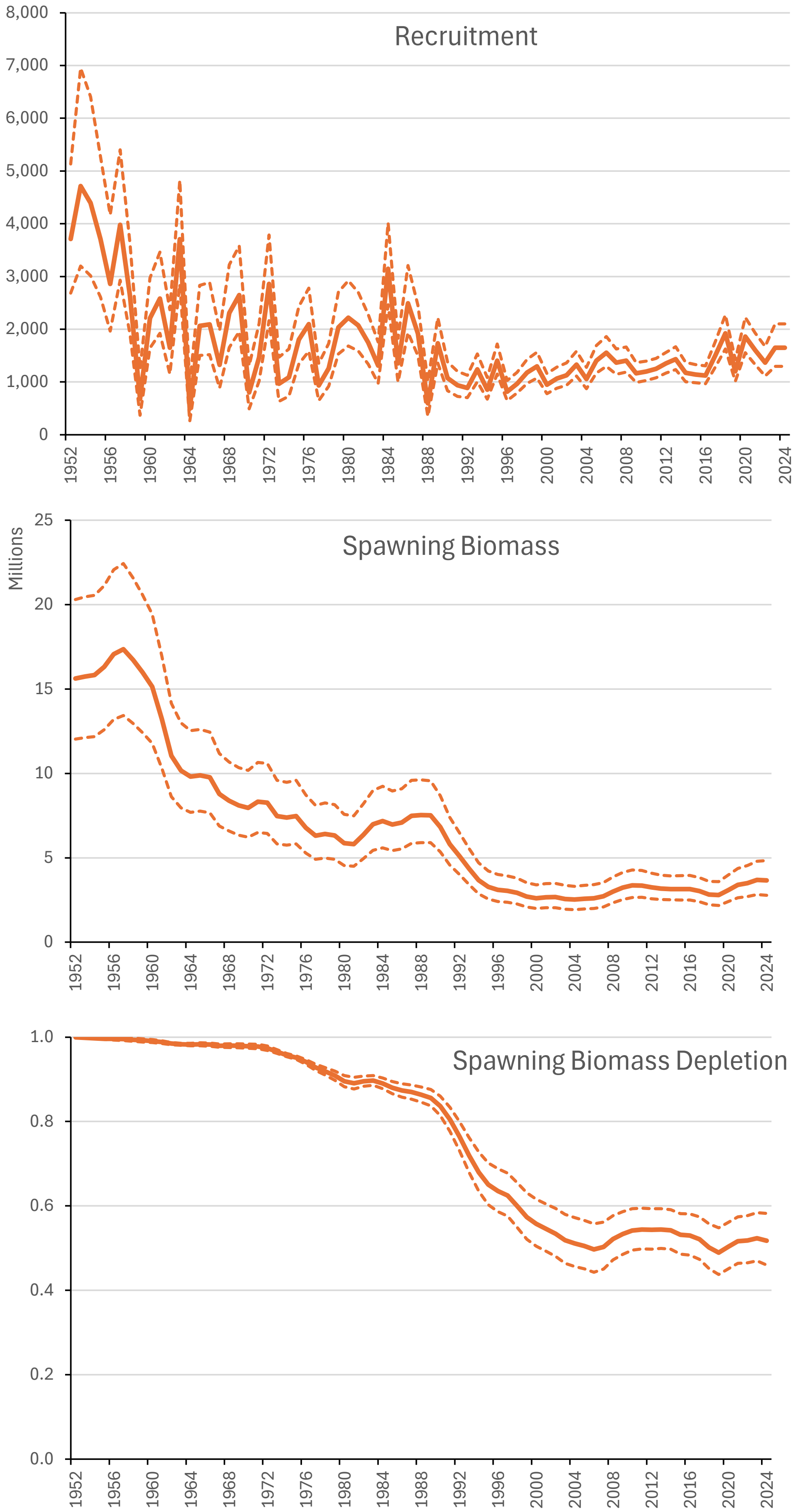

Figure 24. Estimated recruitment, spawning biomass and spawning biomass depletion (solid lines) and estimated 95% confidence intervals (dashed lines) for YELLOWFIN TUNA.

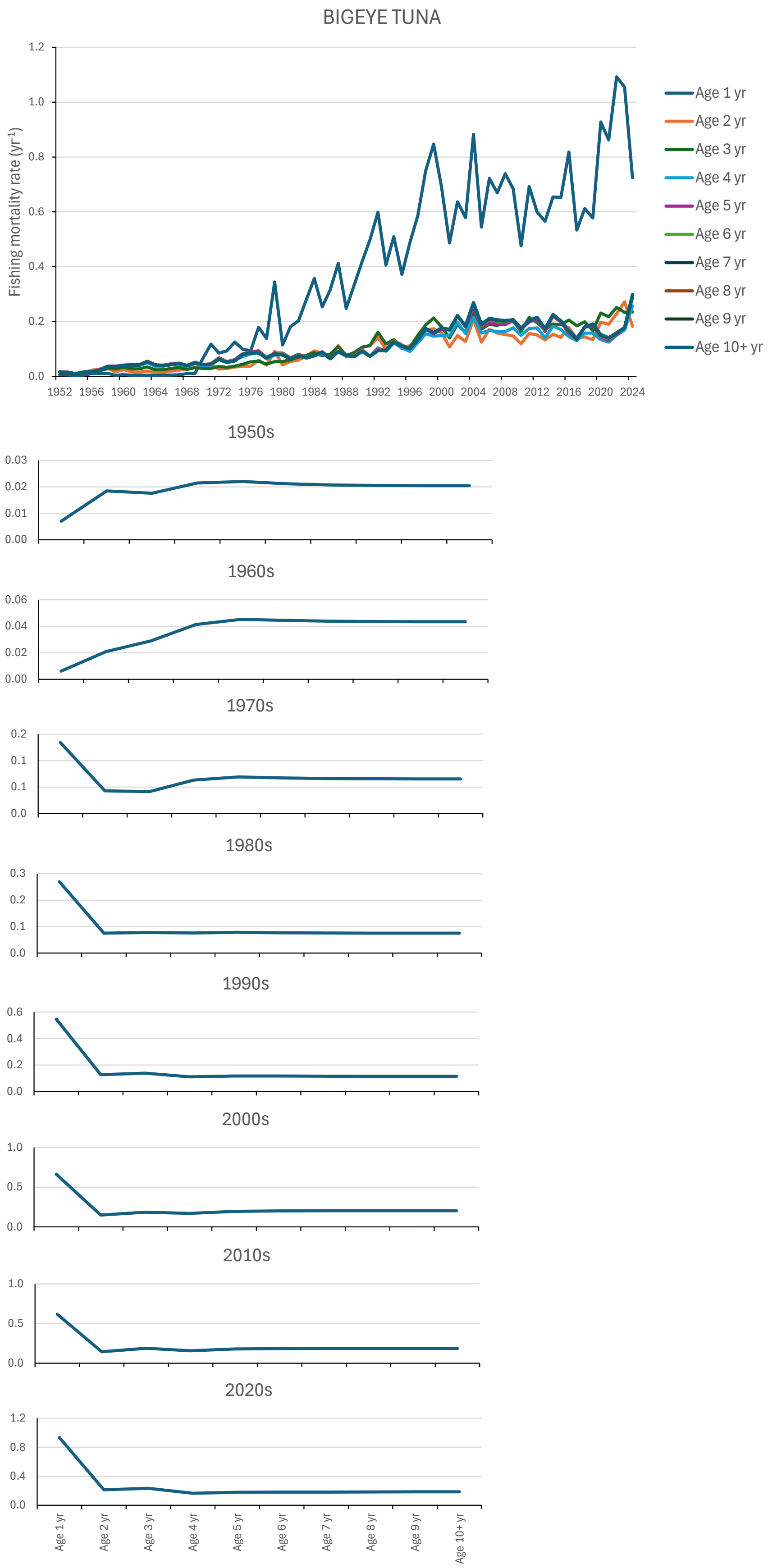

Figure 25. Estimated fishing mortality of BIGEYE TUNA by year (upper plot) and by annual age classes over decade (lower plot).

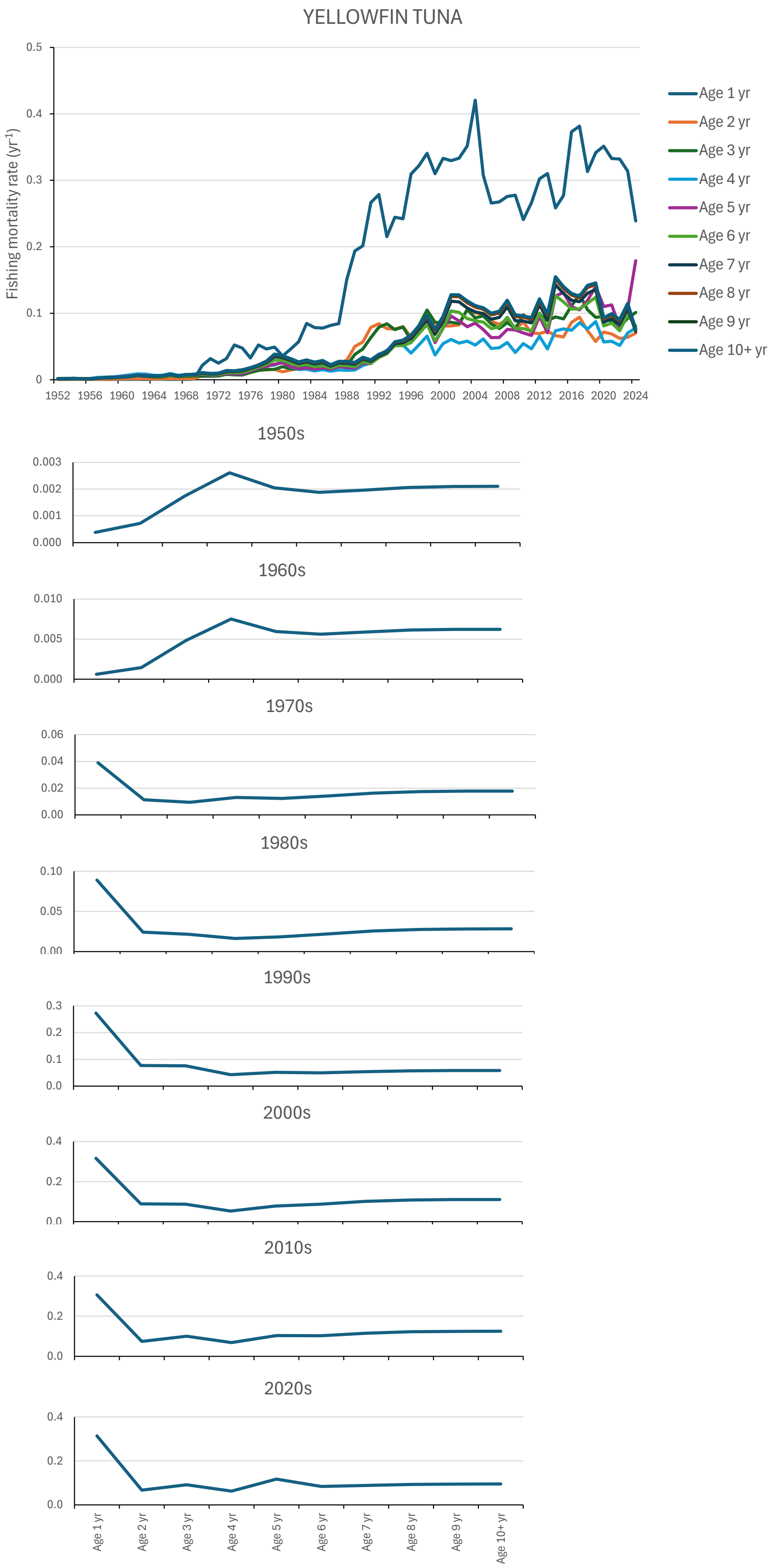

Figure 26. Estimated fishing mortality of YELLOWFIN TUNA by year (upper plot) and by annual age classes over decade (lower plot).

Appendix 1: Single-region models for the tropical region

Single-region models for the tropical region only (regions 2, 3 and 4 in Figure 1) were also implemented for bigeye and yellowfin tuna. The objective was to define a region that:

1. Captured the majority of catches – 75% (82%) of the total WCPO catch for 1952-2024 (2015-2024) for bigeye tuna; and 92% (95%) of the total WCPO catch for 1952-2024 (2015-2024) for yellowfin tuna; and
2. Would likely be more homogeneous with respect to population distribution and critical demographic processes such as growth.

There was insufficient time to fully explore the diagnostics of these models, however we can note that:

1. Model convergence properties were similar to the WCPO models, with maximum parameter gradients <1e-04 and positive definite Hessian matrices;
2. Parameter boundary conditions and high parameter correlation were no more frequent than in the WCPO models;
3. Estimated asymptotic lengths for the growth curves were slightly smaller than those estimated for the WCPO models;
4. Fits to the CPUE indices and aggregate LF data were similar to those of the WCPO models;
5. Fits to the CAAL data sets for fisheries sampled in regions 2, 3 and 4 were slightly improved overall, but still showed evidence of growth heterogeneity among those remaining regions.

A selection of key results for the topical models is shown in Figure 27 for bigeye tuna and Figure 28 for yellowfin tuna. For bigeye tuna, the SB scale was estimated to be slightly higher post-1970 and the extent of SB depletion less than in the WCPO model. While this is a counter-intuitive result, it perhaps demonstrates that population scaling is not particularly well determined in these models, and small changes to model structure can result in significant changes in population scale.

For yellowfin tuna, the results are more intuitive, with a moderately reduced population scale in the tropical model compared to the WCPO model.

In due course, comparison of these results with the spatial assessment models may provide further insights into the performance of these models.

Figure 27. A selection of key results (growth, recruitment, spawning biomass, spawning biomass depletion) from the tropical model for BIGEYE TUNA, compared to the single-region WCPO model (Diagnostic).

Figure 28. A selection of key results (growth, recruitment, spawning biomass, spawning biomass depletion) from the tropical model for YELLOWFIN TUNA, compared to the single-region WCPO model (Diagnostic).

Appendix 2: Comparison of orthogonal polynomial recruitment with “mean+devs” recruitment

The single-region models presented in the paper have used an orthogonal polynomial recruitment (OPR) structure, with a fully saturated year effect (but a common year effect for the terminal two years) and a constant season effect. This recruitment parameterisation was adopted to simplify the models in the expectation of improving their numerical stability. Here we present the top-level results for standard “mean+devs” versions of the bigeye and yellowfin tuna models (with recruitment for the terminal 6 quarters set to the arithmetic mean of the full time series) to verify that they are qualitatively the same.

The “mean+devs” versions took longer to converge than the OPR versions, and did not achieve positive definite Hessian conditions, with one and two negative eigenvalues, respectively, for bigeye and yellowfin tuna models. Nevertheless, the estimates of recruitment, SB and SB depletion are practically identical for the two recruitment formulations for both species (Figure 29).

The authors also discussed the possibility that the OPR structure might be the source of the retrospective bias identified in the models, and so we repeated the retrospective analysis for bigeye tuna using the “mean+devs” recruitment structure. Those results are shown in Figure 30. The results are practically identical to the bigeye tuna retrospective analysis conducted using the OPR structure (Figure 19). Mohn’s ρ statistics for the “mean+devs” retrospective analysis are: recruitment -0.146; SB -0.420; SB depletion -0.385. These values compare closely with the OPR retrospective analysis for bigeye tuna (Table 4). We therefore conclude that the use of OPR is not implicated in producing the retrospective bias observed in these models.

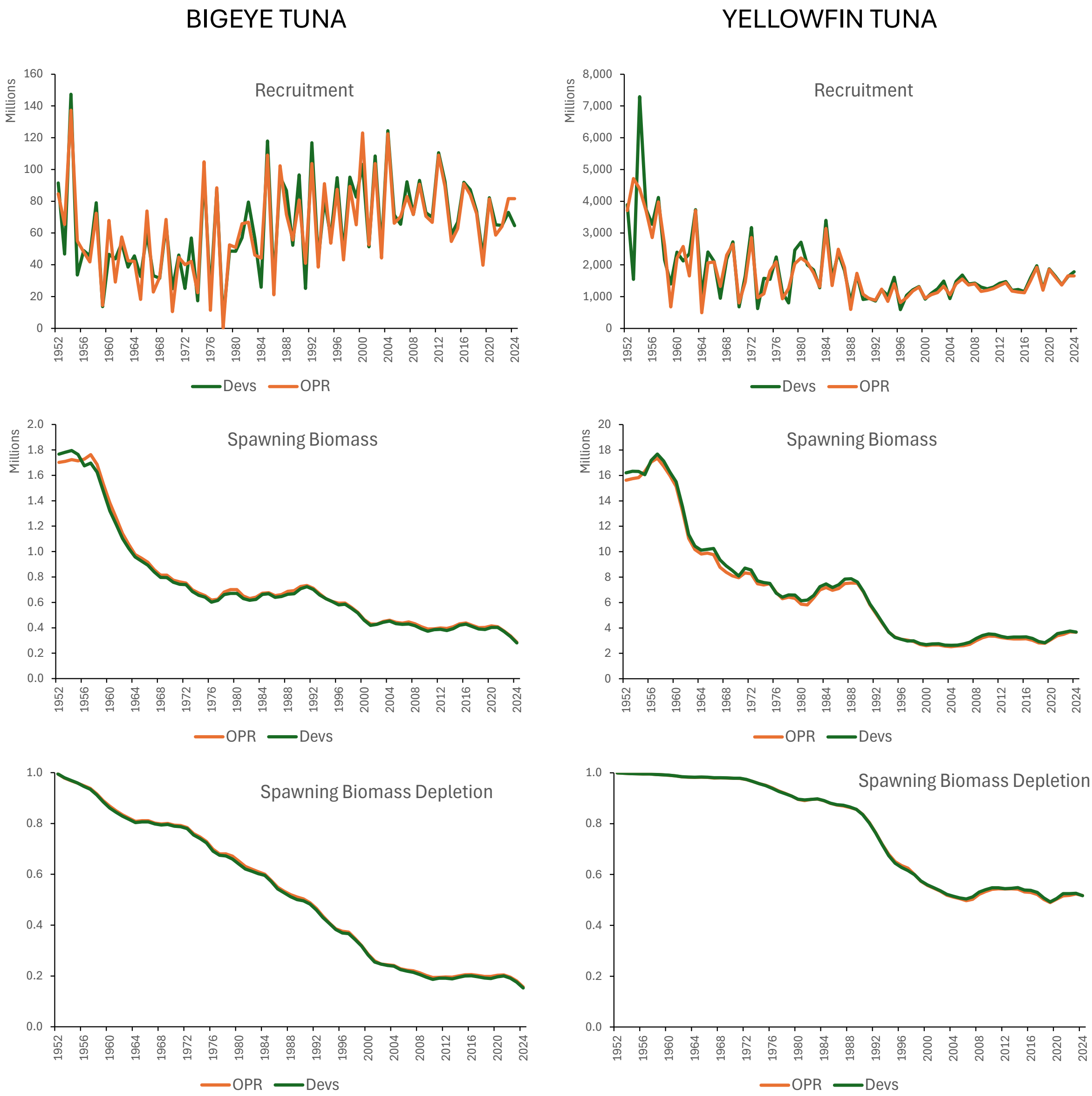

Figure 29. Estimates of recruitment, spawning biomass and spawning biomass depletion obtained from models with the orthogonal polynomial recruitment (OPR) structure and the standard "mean+devs" (Devs) structure for bigeye and yellowfin tuna single-region WCPO models.

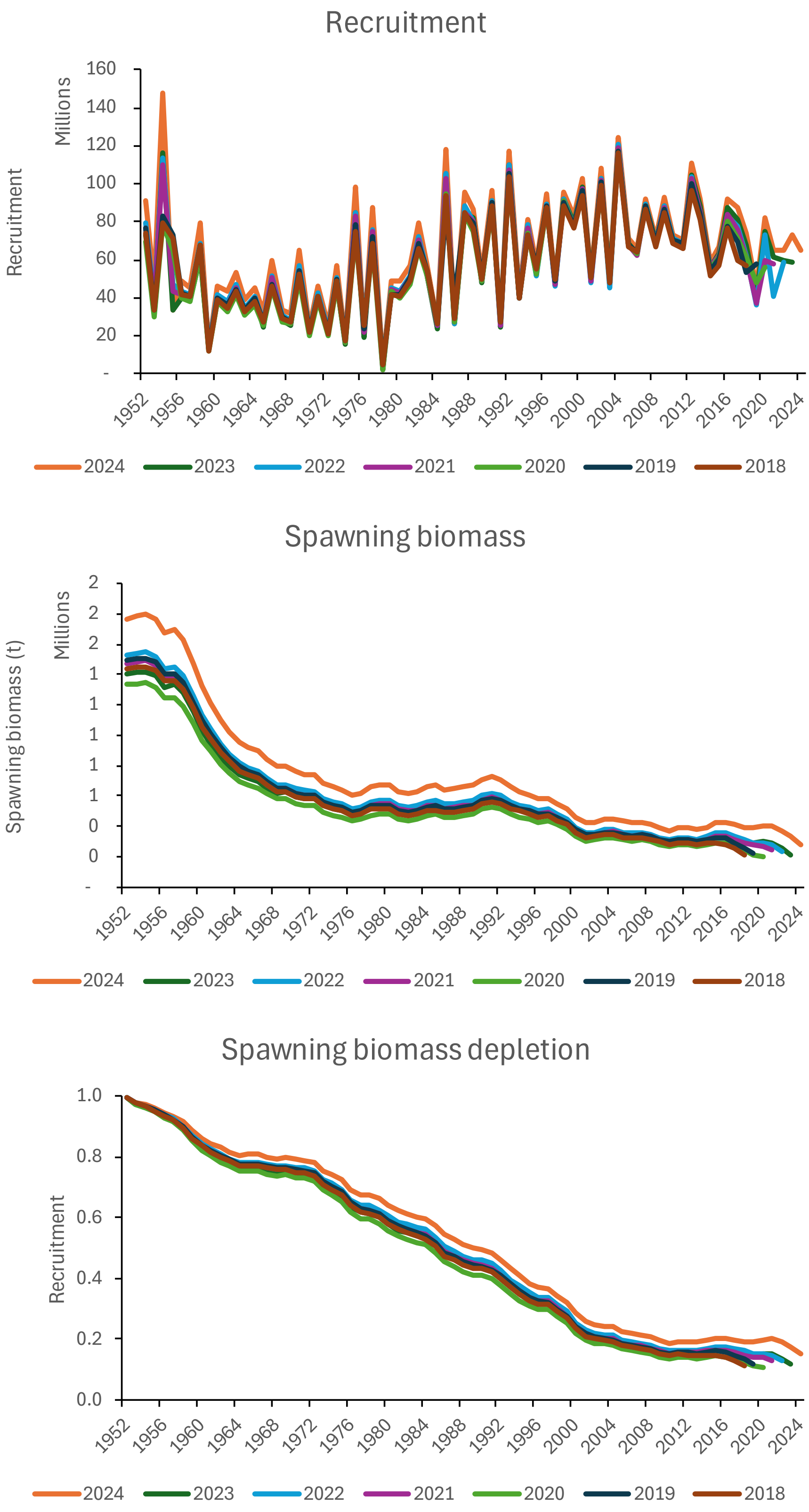

Figure 30. Retrospective analysis for BIGEYE TUNA, using the "mean+devs" recruitment structure.